Aerosol and Air Quality Research, 16: 958–976, 2016

ISSN: 1680-8584 print / 2071-1409 online
doi: 10.4209/aaqr.2015.08.0522

Improving the Representation of Cross-Boundary Transport of Anthropogenic Pollution in East Asia Using Radon-222

Scott D. Chambers[1*], Chang-Hee Kang[2], Alastair G. Williams[1], Jagoda Crawford[1], Alan D. Griffiths[1], Ki-Hyun Kim[3], Won-Hyung Kim[2]

[1] *Australian Nuclear Science and Technology Organization, Locked Bag 2001 Kirrawee DC NSW 2232, Australia*
[2] *Department of Chemistry, Jeju National University, Jeju 690–756, Korea*
[3] *Department of Civil & Environmental Engineering, Hanyang University, 222 Wangsimni-Ro, Seoul 133-791, Korea*

ABSTRACT

We report on 10 years of hourly atmospheric radon, CO, and SO_2 observations at Gosan Station, Korea. An improved radon detector was installed during this period and performance of the detectors is compared. A technique is developed whereby the distribution of radon concentrations from a fetch region can be used to select air masses that have consistently been in direct contact with land-based emissions, and have been least diluted *en route* to the measurement site. Hourly radon concentrations are used to demonstrate and characterise contamination of remote-fetch pollution observations by local emissions at this key WMO GAW site, and a seasonally-varying 5-hour diurnal sampling window is proposed for days on which diurnal cycles are evident to minimise these effects. The seasonal variability in mixing depth and "background" pollutant concentrations are characterised. Based on a subset of observations most representative of the important regional fetch areas for this site, and least affected by local emissions, seasonal estimates of CO and SO_2 in air masses originating from South China, North China, Korea and Japan are compared across the decade of observations.

Keywords: ^{222}Rn; Fetch analysis; Local effects; Model benchmarking; Sampling window.

INTRODUCTION

Anthropogenic emissions from urban or industrial regions are integrated by, and mixed within, the atmospheric boundary layer (ABL). In the absence of major removal mechanisms such as synoptic fronts and deep convection (e.g., Williams *et al.*, 2009, 2011), the constituents not subject to dry/wet deposition or chemical transformation can remain within the ABL long enough to travel significant distances and into different geo-political regions (Guttikunda *et al.*, 2001; Kim *et al.*, 2007b; Choi *et al.*, 2008; Lin *et al.*, 2008; Song *et al.*, 2008; Begum *et al.*, 2011). This issue is particularly pertinent in the northeast Asian region, where political boundaries are close and rapid industrialisation, economic growth and increasing energy and transport demands from the large and growing populations have resulted in a disproportionately large fraction of global anthropogenic emissions in recent decades (Perry *et al.*, 1999; Guttikunda *et al*., 2001; Streets *et al.*, 2003; Lin *et al.*, 2008; Sahu *et al.*, 2009; Hu *et al.*, 2014).

The best understanding of potential climatic, ecological and health effects associated with anthropogenic emissions is generally achieved with chemical transport models coupled to detailed emission inventories and remote sensing data. To improve the accuracy of model simulations, results are evaluated against ground-based measurements with a view to iterative enhancement of model representations or assimilated inventory data (Huebert *et al.*, 2003). To minimise the chance of misleading comparisons, it is of critical importance to ensure that the ground-based reference observations are well matched with the model output, especially with respect to the fetch regions of interest.

In order to derive quantitative information about emissions from a fetch region based on downstream ground-based observations, it is necessary to: (i) understand the measurement "footprint", (ii) identify measurement periods most representative of air masses that have been in direct contact with the surface over which they have travelled, and have not been significantly diluted by synoptic fronts or deep convection in transit, (iii) ensure that the ground-based measurements are representative of the whole ABL (e.g., not isolated from remote sources by the nocturnal inversion), (iv) minimise any contamination of observations by local emissions, (v) adequately characterise diurnal and seasonal changes in the ABL mixing depth at the observation site, and (vi) be able to characterise the evolving large-

* Corresponding author.
Tel.: +612-9717-3058
E-mail address: szc@ansto.gov.au

scale (global or hemispheric) "background" pollutant concentrations that are unrelated to regional emissions but may have interannual or even seasonal variations.

In this study, we use a combination of radon and trajectory analyses to address the abovementioned requirements at Gosan Station, a World Meteorological Organisation (WMO) Global Atmosphere Watch (GAW) site in South Korea. Based on this analysis, we propose an easy-to-implement selection strategy for identification of those sampling periods that can be best used to characterise emissions from the important regional fetch areas for this site. To facilitate future comparison studies, the technique is then applied to a 10-year period (2001–2010) of anthropogenic trace gas observations at Gosan that, in whole or in part, has been the focus of numerous previous investigations (e.g., Huebert *et al.*, 2003; Park *et al.*, 2004; Nakajima, 2007; Kang *et al.*, 2009; Sahu *et al.*, 2009; Zhang *et al.*, 2009; Kim *et al.*, 2011; Crawford *et al.*, 2015).

METHODS

Site and Setting

Gosan station (33.29°N, 126.16°E; 70 m above sea level, a.s.l.) is situated on the west coast of Jeju, a volcanic island centred about Mount Halla (1950 m a.s.l.). Compared to mainland Korea, Jeju is sparsely populated with little industrial activity, so the main anthropogenic pollution sources are: China (500 km west), Kyushu, Japan (200 km east), and mainland Korea (100 km north).

Since Jeju is in the Asian pollution "outflow" region (20–50°N; e.g., Talbot *et al.*, 1997; Kim *et al.*, 2014a), Gosan is ideally situated to observe low-level (boundary layer) monsoonal transport of emissions, and has been a "super site" in numerous campaigns (Huebert *et al.*, 2003; Kim *et al.*, 2007a; Choi *et al.*, 2008). Furthermore, when not in the path of outflow events, Gosan is considered an ideal "background" monitoring site (Park *et al.*, 2004; Kang *et al.*, 2009; Kim *et al.*, 2011; Kim and Shon, 2011).

Atmospheric Radon Observations

Radon-222 (radon) is a naturally-occurring unreactive and poorly-soluble radioactive gas sourced mainly from unsaturated or unfrozen terrestrial surfaces. Consequently, it is an unambiguous indicator of recent terrestrial influence on air masses (e.g., Balkanski *et al.*, 1992; Chambers *et al.*, 2014). Its half-life (3.8 d) is much longer than the ABL mixing timescale (~1 hour), but short enough compared to large atmospheric processes to constrain concentrations in the troposphere to 1–3 orders of magnitude below near-surface values (e.g., Liu *et al.*, 1984; Williams *et al.*, 2011). These physical characteristics make radon an ideal tracer of atmospheric transport and mixing processes (e.g., Williams *et al.*, 2009, 2013; Chambers *et al.*, 2014, 2015a).

As part of the Asian Aerosol Characterisation Experiment (Huebert *et al.*, 2003) a 750 L dual flow-loop two-filter radon detector (Whittlestone and Zahorowski, 1998) was installed at Gosan in late 2000 (see Zahorowski *et al.*, 2005 for details). By similar methods to those reported in Chambers *et al.* (2014), the detector's instrumental background was checked four times a year by shutting down flow through and within the detector for 24 hours, and monthly calibrations were performed by injecting radon at 80 cc min^{-1} from a Pylon source (18.5 ± 4% kBq Radium-226) for 5 hours. The net peak detector count rate was then related to the concentration of radon within the detector, calculated as the ratio between the source radon delivery rate (2.331 Bq min^{-1} ^{222}Rn) and the sampling flow rate. The coefficient of variability (CoV) for calibrations each year was 4–6%.

In July 2007, the detector was upgraded to a 1500 L model, resulting in an improved lower limit of determination (LLD; from 0.09 to 0.04 Bq m^{-3}), increased sensitivity (from 0.223 to 0.295 counts per second/(Bq m^{-3})), and an improved calibration stability. The sampling height was also increased from 5 to 10 m a.g.l. Here the LLD is defined to be the concentration for which the counting error reaches 30%. Counting error reduces with increasing concentration such that, at ambient concentrations of 3 Bq m^{-3}, the error is < 2%. Considered in conjunction with the calibration CoV and manufacturer's quoted source accuracy (± 4%), the measurement uncertainty at 3 Bq m^{-3} is < 12% (0.36 Bq m^{-3}).

Pollution and Climatology Observations

Aerosol and trace gas sampling was conducted by the Korean Ministry of Environment from 6 m a.g.l., and meteorological observations were conducted nearby by the Korean Meteorological Administration (see Kim *et al.*, 1998 and Kim *et al.*, 2011 for details). For the purposes of this study (demonstrating a data selection method) we will focus only on sulphur dioxide (SO_2) and carbon monoxide (CO), often used as indicators of anthropogenic activity.

CO primarily derives from incomplete combustion processes. Its residence time (0.1 year, Weinstock, 1969) is comparable to radon, enabling transport over large distances. SO_2, a product of fossil-fuel combustion, is considered to be one of the most individually important precursor compounds for secondary matter in the atmosphere (Guttikunda *et al.*, 2001; Zhang *et al.*, 2004). Once emitted, SO_2 typically converts to sulphate (SO_4^{2-}) at a rate of ~1% h^{-1} (Seinfeld and Pandis, 2006).

CO measurements were made by NDIR absorption (Thermo Environmental Instruments, model 48C, USA), for which the detection limit was 0.04 ppm and a precision was 10%. SO_2 was measured by UV fluorescence (Thermo Environmental Instruments, model 43C–TL, USA) with a detection limit of 0.1 ppb (60 sec avg. time) and a precision of 10% (Sahu *et al.*, 2009). Both instruments were calibrated quarterly.

While pollution has been monitored at Gosan for over two decades (Kim *et al.*, 1995; Carmichael *et al.*, 1997; Park *et al.*, 2004; Kang *et al.*, 2009; Kim *et al.*, 2014b), here we consider only the initial decade of overlapping radon and trace gas observations (Jan 2001–Dec 2010).

Air mass back trajectories used in this study were calculated using the PC version of HYSPLIT v4.0 (HYbrid Single-Particle Lagrangian Integrated Trajectory; Draxler and Rolph, 2003), with a starting height of 200 m (see Crawford *et al.*, 2015 for further details). All times reported are local (LST = UTC + 9 h), and the northern hemisphere

seasonal convention is used.

RESULTS AND DISCUSSION

Radon Observations

Daily-mean radon concentrations varied from 0.04–7 Bq m^{-3} (Fig. 1), and the seasonal cycle was characterised by a winter maximum and late summer minimum (Fig. 2). Monthly statistics for the composite 10-year period are provided in Table 1 for (i) all hourly data, and (ii) data within the diurnal sampling window (defined below under "Influences of local emissions and diurnal mixing"), to serve as a benchmarking tool for models incapable of adequately resolving local mixing or island effects on diurnal timescales.

Since the July 2007 detector changeover, reported mean annual radon concentrations dropped by ~14% with little change in the amplitude of the seasonal cycle (Fig. 3). This is attributable to a combination of measurement uncertainty, the change in sampling height, changes in detector characteristics not captured by the calibration process, and refurbishment of the calibration system. While this change in performance is of no consequence to the air mass categorisations performed in this study, data may need to be adjusted accordingly for other applications.

Representativeness of Remote Fetch regions

The seasonality of Gosan's terrestrial fetch has been well documented (Guttikunda *et al.*, 2001; Park *et al.*, 2004; Zahorowski *et al.*, 2005; Kim *et al.*, 2014a). The maximum terrestrial influence (October through February; Fig. 2) occurs under strong, consistent conditions of outflow from the Asian continent with a fetch that includes the Korean Peninsula and North China (Fig. 4(b)). Minimum terrestrial

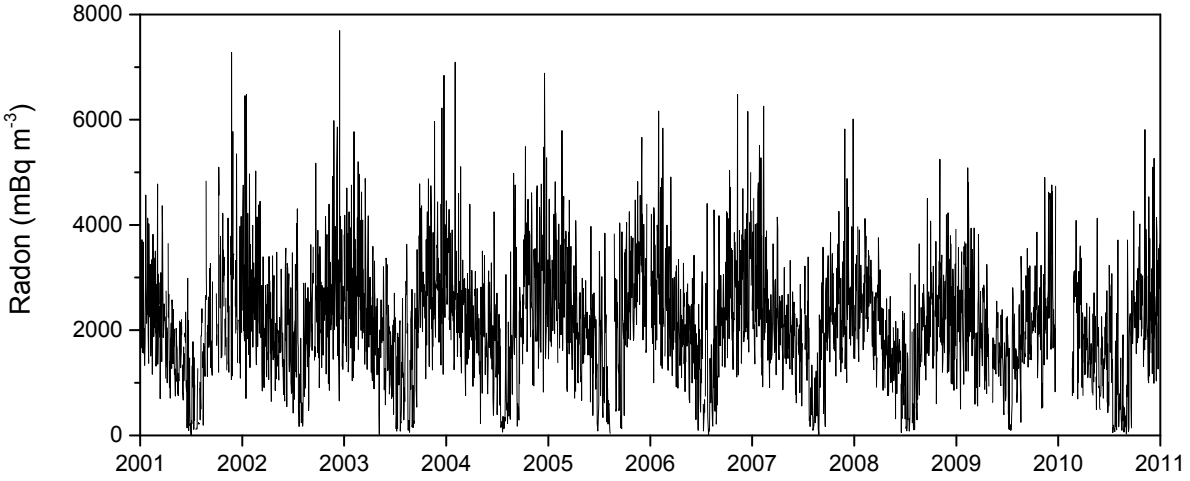

Fig. 1. Daily-mean Gosan radon based on seasonally–varying 5-hour diurnal sampling window (see Section 3.3 for window definition).

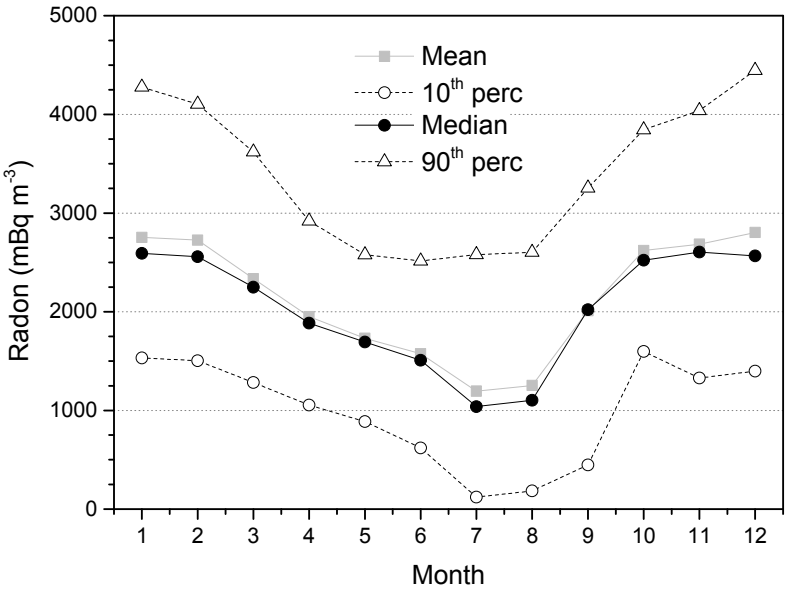

Fig. 2. Composite monthly mean and distributions of Gosan daily-mean radon over a 10-year period, based on the 5-hour diurnal sampling window.

Table 1. Monthly means, standard deviation and distributions of radon concentration (mBq m^{-3}) for a composite year based on hourly data between 01 Jan 2001 and 31 Dec 2010.

Statistics based on all hourly data								
Month	Radon	N	σ	10th	25th	50th	75th	90th
1	2957.7	6265	1218	1605.6	2069	2762	3616.8	4617.6
2	2951.8	6114	1174	1621.1	2126	2784.9	3589	4541.1
3	2565.4	7275	1044	1368.8	1813.1	2418.1	3174.8	3985.6
4	2269.1	6931	904	1211.2	1650.2	2150.6	2756.8	3438.7
5	2038.8	7065	927	1028.3	1410.4	1908.6	2478.3	3263.2
6	1973.1	7017	1173	700.6	1227.7	1770	2497.7	3455.1
7	1516.7	6793	1293	183.4	420.8	1241.1	2254.6	3197.9
8	1845.5	6884	1444	267.6	628.5	1610	2657.5	3715.4
9	2455.2	6574	1258	739.5	1681.8	2396.7	3186.4	3981
10	3002.3	7168	1063	1791.3	2280.8	2837.3	3627.9	4369.8
11	3004	6962	1241	1544.3	2126.5	2871.6	3704.2	4615
12	2945.8	6732	1257	1510.9	2018.8	2740.5	3669.9	4613.9
Mean	2453.3	81780	1276.6	914.9	1599.1	2328.5	3172.7	4110.5
Statistics based only on data from within a 5-hour diurnal window each day								
Month	Radon	N	σ	10th	25th	50th	75th	90th
1	2783.5	1592	1110	1550.2	1982.1	2602.6	3399	4336
2	2735.9	1536	1083	1502.7	2003.4	2559.1	3283.7	4170.5
3	2336.9	1826	915	1277.5	1725.8	2253.9	2832	3622
4	1951.9	1744	705	1069.5	1432.6	1886	2377.2	2911.8
5	1723.9	1772	673	886	1262.8	1691.1	2104.2	2539.9
6	1560.2	1756	780	620.4	1025.1	1488.1	2032	2512.3
7	1187.5	1685	978	123.6	274.7	1038.3	1903.8	2555.5
8	1251	1717	968	180.5	419.5	1097.7	1881.4	2603.5
9	2010.9	1659	1012	451.9	1464.9	2014	2640.8	3260.2
10	2628.1	1782	881	1598.5	2009.8	2524.7	3143	3846.7
11	2709.4	1725	1134	1341.6	1904.7	2622	3278.6	4084.2
12	2812.8	1683	1255	1391.8	1935.8	2588.5	3484.6	4436.9
Mean	2132.9	20477	1128.6	722	1392	2045.1	2757.2	3578.8

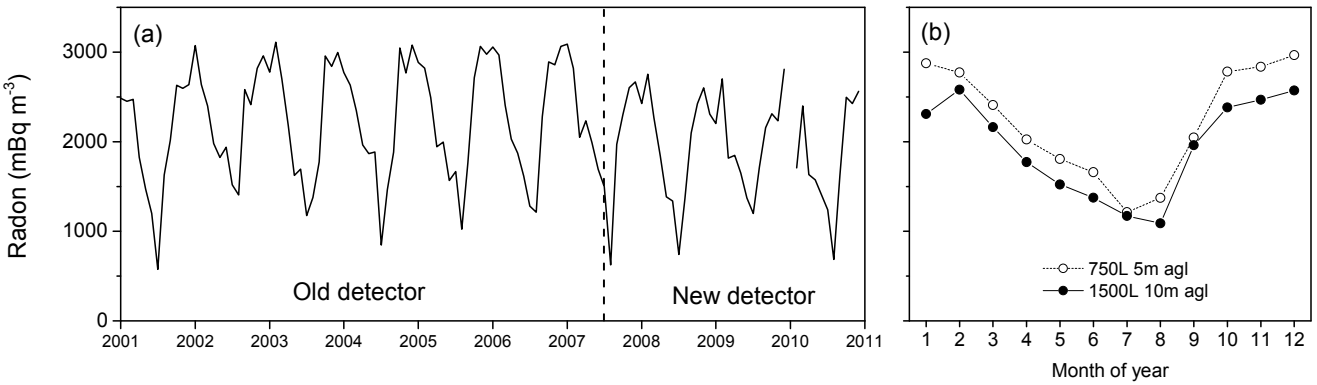

Fig. 3. (a) Monthly mean radon based on the 5-hour diurnal sampling window, and (b) comparison of radon between old and new detectors (based on 6-year and 3-year composites, respectively).

influence (July and August), on the other hand, usually occurs at the height of the summer monsoon (onshore flow), when fetch is mainly from the western Pacific (Fig. 4(a)). However, "oceanic" air masses (nominally, radon < 100 mBq m^{-3}) can occur anytime from early-May to late-September.

Back-trajectory analyses were used to categorise "terrestrial" fetch regions by composite month in Fig. 5(a). In winter, the dominance of Korean and North China air masses is clearly evident, whilst the "transitional" months (March–June, and September; Fig. 2) were characterised by mixed fetch conditions. The more gradual spring transition included a larger contribution from South China than the rapid autumn transition, which included more Japanese fetch. The influence of "oceanic" air masses (those that had not made landfall in 5 days prior to reaching Gosan), shown

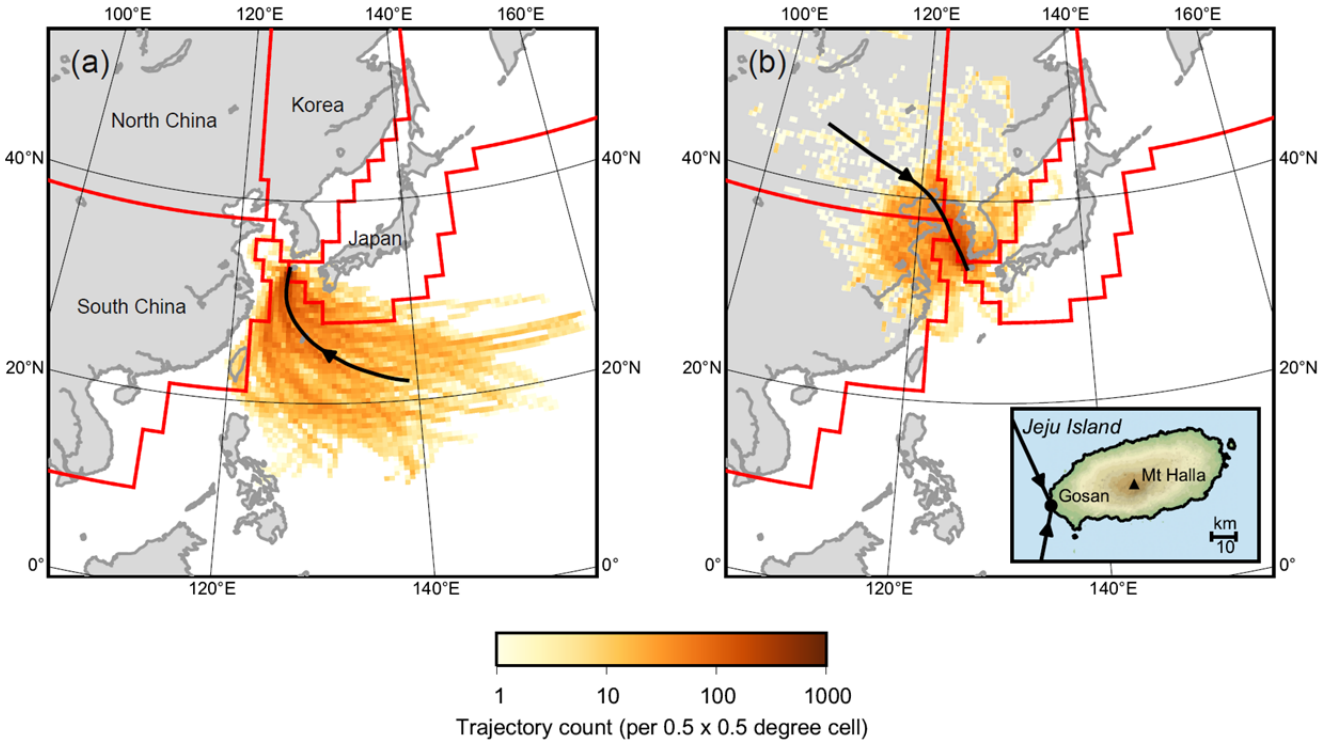

Fig. 4. Density functions based on hourly 4-day HYSPLIT v4.0 back-trajectories from within the 5-hour diurnal sampling window for (a) low-radon summer events, and (b) high-radon winter events. Inset shows Jeju Island with location of Gosan Station.

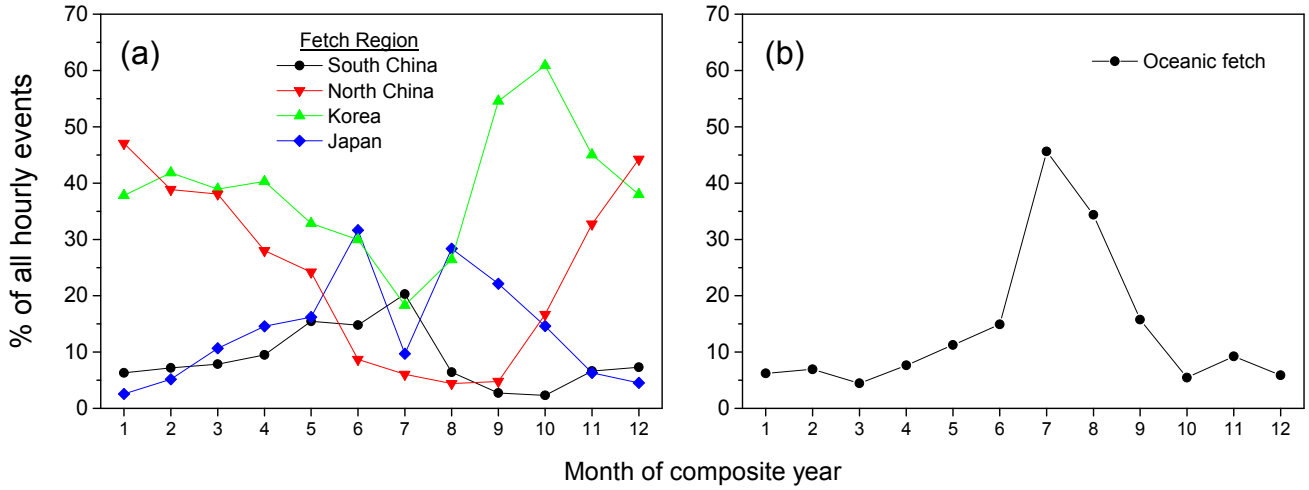

Fig. 5. Monthly breakdown of relative fetch contributions (as a percentage of all hourly events) to Gosan air masses averaged over the 10-year dataset for (a) terrestrial and (b) oceanic fetch.

separately in Fig. 5(b), is clearly dominant in the summer months. The slight increase in radon from July to August (Fig. 2) was attributable to a switch from southerly (Jeju Island fetch < 3 km) to southeasterly air masses (Jeju Island fetch 15–30 km), and an increased fetch over Japan and Korea.

Fetch regions are often assigned solely by trajectory analyses based on model output in two (or perhaps three, if altitude is included) spatial dimensions. Such representations of recent fetch history alone may not be sufficient to accurately diagnose the degree of contact an air mass has had with surface-based pollution sources, however. Even when model trajectories can be considered reliable, there is no guarantee that an air mass has been in direct contact with the land surface; for this reason, the use of model trajectories in conjunction with a measured terrestrial tracer such as radon gives more definitive results (e.g., Crawford *et al.*, 2009). Radon's physical characteristics ensure that an air mass' radon concentration will be closely linked to terrestrial influence over the past 2–3 weeks. For a given fetch

(assuming a uniform radon flux), the higher an air mass' radon concentration, the longer it has spent in contact with surface sources, or the less dilution it has been subjected to *en route* to Gosan. Therefore, the more likely observations are to be representative of surface-based emissions over that fetch. Here, "dilution" is understood to be a result of either (i) tropospheric injection, during fronts or other severe weather events, or (ii) deep convection, which can vent anthropogenic pollutants to the troposphere (e.g., Williams *et al.*, 2009, 2011).

With the above in mind, pollution fetch analyses for this study were performed in two steps. Firstly, northeast Asia was coarsely divided into four regions (South China, North China, Korea and Japan; Fig. 4(a)) in a similar manner to Park *et al.* (2004). Fetch regions were then assigned according to an air mass' mean location during its most recent 24 hours over land prior to reaching Gosan. Secondly, to produce observations most representative of emissions from each fetch region, we (i) selected only observations within the 5-hour diurnal sampling window (defined in the next section) to exclude local influences and mixing effects, (ii) calculated composite monthly radon distributions for each fetch, and (iii) selected only the high radon events, by excluding air masses with radon below the monthly median for each fetch. This third step assumes that low radon events are poorly representative of surface-based sources due to dilution or limited interaction with the corresponding ABL. It also assumes a uniform radon flux *within* each region, whilst allowing for the possibility of variability in flux *between* regions.

Influences of Local Emissions and Diurnal Mixing

Although sparsely populated, under certain conditions local emissions from Jeju Island can contaminate Gosan pollution observations (e.g., Kim *et al.*, 1998). To ensure measurements are as representative as possible of remote fetch regions, it is important to determine: (a) whether contamination by local emissions is significant, (b) the conditions under which local influences actually become problematic, and (c) a suitable sampling strategy to minimise these influences.

Near-surface observations are contributed to by both large- and local-scale emissions. The maximum large-scale contributions occur during the day, when the ABL is well mixed, whereas the maximum local-scale contribution occurs at night, when the nocturnal inversion can completely isolate the near-surface air from the deeper layer above and therefore also from the larger-scale signal (e.g., Williams *et al.*, 2013; Chambers *et al.*, 2015b). The chemical compositions of the nocturnal boundary layer (NBL) and residual layer above evolve largely independently until sunrise, when convective mixing reconnects them.

At Gosan, seasonal mean radon (e.g., straight dashed lines in Fig. 6) indicates the potential for influence from large-scale terrestrial-based sources, whereas diurnally, radon concentrations respond to the changing local mixing depth. Fig. 6 therefore demonstrates a decreasing potential for large-scale pollution contributions from winter to summer, and corresponding increase in the potential for contamination of observations by local-scale emissions as diurnal mixing depth changes become more pronounced. However, even in summer the diurnal amplitude of radon at Gosan (~1.2 Bq m^{-3}) is more than an order of magnitude less than observed at a flat, inland site (e.g., Chambers *et al.*, 2015b), demonstrating the stabilising oceanic influence on Gosan mixing depths year round.

Of particular interest in Fig. 6 is the build-up of radon before dawn in all seasons. Assuming a negligible oceanic radon flux (Zahorowski *et al.*, 2013), this demonstrates a local-scale contribution to Gosan observations, since mean nocturnal winds are too small to bring radon from neighbouring source regions (China, Korea or Japan) over the course of a single night. To investigate the possibility of similar local influences on pollution observations we analysed diurnal cycles of CO and SO_2 (Fig. 7).

The CO diurnal cycle was also characterised by a morning maximum, afternoon minimum, and nocturnal build-up phase. In summer, once the NBL was well established (around 2100 h) there was a gradual accumulation of CO (~0.0013 ppm h^{-1}) until sunrise. In winter, however, when

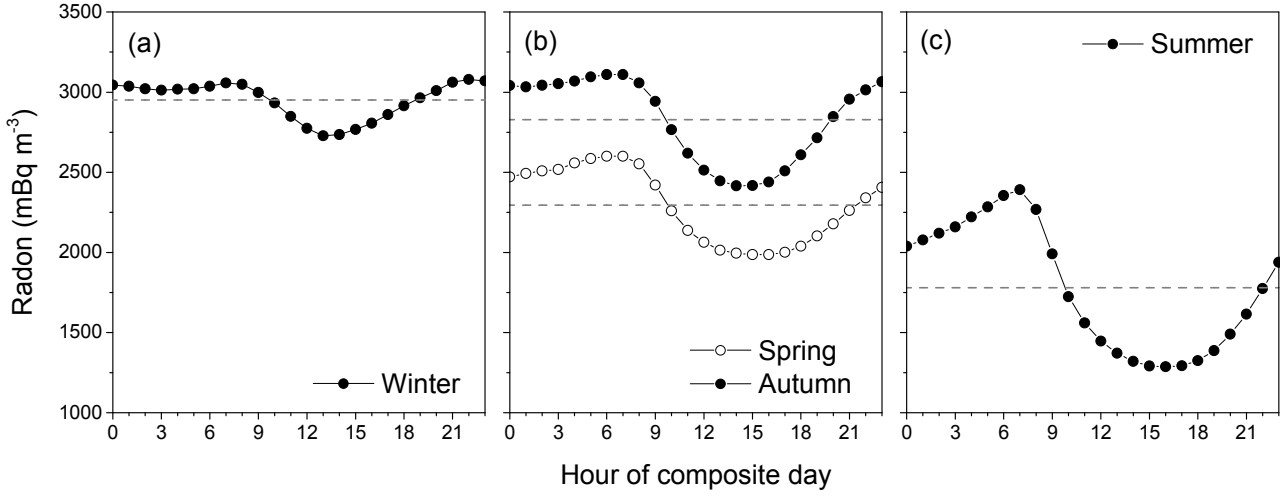

Fig. 6. Diurnal composite Gosan radon concentration by season.

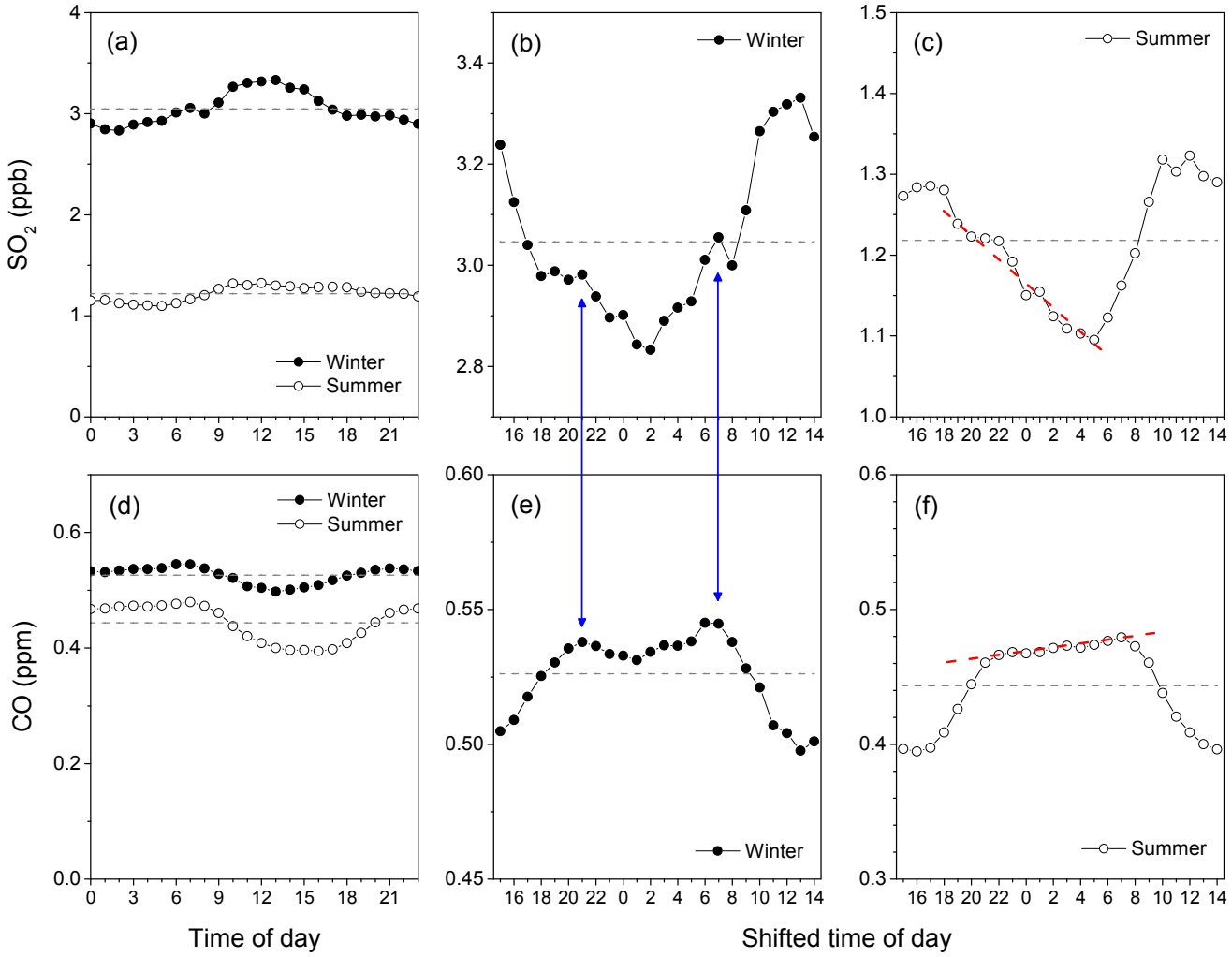

Fig. 7. Composite hourly-mean diurnal cycles of SO_2 and CO in winter and summer: (a, d) combined on shared ordinate axes, to show relative seasonal changes, and (b, c, e, f) on individual ordinate axes for each season, with time (abscissa) shifted to emphasise nocturnal characteristics.

combustion heaters are commonly used, the nocturnal CO accumulation was more variable, with peaks between 2000–2200 h and 0600-0700 h (Fig. 7(e)). These results confirm local emissions can influence near-surface Gosan CO observations when the atmosphere is poorly mixed, and that the magnitude of this influence changes seasonally.

The SO_2 diurnal cycle was out of phase with CO and radon, characterised by maximum values around noon and minimum values at night. The lack of nocturnal SO_2 accumulation likely indicates a lack of substantial local SO_2 sources (c.f. remote source magnitudes; e.g., Kim *et al.*, 1998; Park *et al.*, 2004; Sahu *et al.*, 2009). In summer, residual SO_2 trapped in the NBL when it formed slowly reacts or deposits, causing a gradual decline in concentrations between sunset and sunrise (Fig. 7(c)). The rate of this decline (0.0167 ppm h^{-1}, or 1.3% h^{-1} relative to the afternoon average) is similar to the 1% h^{-1} conversion rate proposed by Seinfeld and Pandis, (2006). In winter, however, the nocturnal SO_2 behaviour was more variable; primarily due to local combustion emissions, as evident by the correspondence with CO peaks (blue arrows at 2100 h and 0700 h in Fig. 7).

While daily mean observations could be used to assess the impact/exposure of Gosan residents or ecosystems to the combined effects of remote and locally-produced pollutants, Fig. 7 shows that, on days when a diurnal cycle exists, Gosan daily means may not be representative of regional-scale outflow pollution characteristics. To better characterise the anthropogenic signature from distant sources in such cases it is necessary to employ a diurnal sampling window restricted to the period when observations are most representative of the whole ABL (see also Zahorowski *et al.*, 2005 and Zhu *et al.*, 2012).

For CO, observations between 1300–1700 h (1100–1600 h) in summer (winter) were most representative of remote sources. Compared to averages over these windows, local sources enhanced nocturnal CO concentrations by 6.6% in winter and 18.8% in summer (the seasonality in the apparent local influences here reflects more the seasonality in nocturnal mixing depth than that of local sources). Thus, a daily-mean CO would, on average, overestimate remote source contributions by 4.2% in winter and 10.5% in summer. For SO_2 the 1000–1800 h (1000–1500 h) summer (winter)

window was most representative of remote emissions. Using daily-means of SO_2 values would, on average, underestimate emissions from remote sources by 7.3% in winter and 5.9% in summer.

Aerosol samples at Gosan (and many similar sites) have been integrated over 24-hour periods (e.g., Park *et al.*, 2004; Crawford *et al.*, 2007; Kim *et al.*, 2011). Hourly Gosan PM_{10} observations (not shown) indicated that daily mean values may underestimate total mass by ~3% by including the nocturnal period dominated by local sources; the effect may be more significant for finer aerosol fractions. Perhaps more importantly, the elemental composition of aerosols collected when observations are most representative of remote sources could be quite different than that for 24-hour samples that include a substantial local-source component. Reducing aerosol integration times to four 6-hour periods daily would enable this problem to be minimised.

Based on a combination of the findings above we propose a seasonally-varying 5-hour diurnal sampling window for Gosan observations to best represent remote emissions: 1100–1500 h LST (inclusive) for Asian outflow conditions (winter monsoon), and 1300–1700 h LST (inclusive) otherwise, when Gosan fetch incorporates more of Jeju Island.

To scale-up results derived using this windowing technique it would be necessary to assume no diurnal variability in remote emissions. We acknowledge the possibility of diurnal variability in remote emissions that this technique will not capture. However, individual sources within the remote regions are spatially dispersed (spread over 10s to 100s of km), and their combined emissions would further disperse over their 100–600 km (1–3 day) journey to Gosan. So any of the original diurnal variability of the individual source strengths that remained in the Gosan ABL at the time of measurement would likely be much less than that caused by local mixing effects.

A further advantage of reporting statistics of ground-based observations for periods when the ABL is well-developed is they are better suited to model evaluation, since model spatial or vertical resolution may be insufficient to resolve the stable NBL or local island effects.

Seasonality of the Gosan ABL Depth

There are two pathways by which atmospheric pollutants leave continental Asia: at high altitude (in the troposphere) following uplift by cold fronts or deep convection, or near the surface, within the ABL (e.g., Kritz, 1990; Balkanski *et al.*, 1992; Crawford *et al.*, 1997). While natural aerosols have been observed at a wide range of altitudes (extending to almost the tropopause; Huebert *et al.*, 2003 and references therein), when not influenced by deep-convection, anthropogenic pollutants are predominantly contained within the ABL (e.g., Huebert *et al.*, 2003; Reid *et al.*, 2013). Thus, if the mixing depth is known at the measurement point, column-integrated pollution estimates can be made and related to regional emissions (Williams *et al.* 2009).

For pollutants in a well-mixed ABL, near-surface concentrations vary strongly as a function of mixing depth (see also previous section). At Gosan there are pronounced seasonal changes in average mixing depth tied to the behaviour of the marine boundary layer (MBL) surrounding Jeju. Seasonal MBL variability is driven primarily by the difference in temperature between the ocean surface and overlying air masses (greatest in winter, least in summer).

The mixing depth at Gosan has been reported to vary between 500 to 1500 m under Asian outflow conditions (Talbert *et al.*, 1997; Kim *et al.*, 2005; Kim *et al.*, 2012; Reid *et al.*, 2013). In lieu of observations we used planetary boundary layer (PBL) depths taken from the NCEP Climate Forecast System Reanalysis (Saha *et al.*, 2010a, b) to estimate the MBL depth within an oceanic grid-cell immediately west of Jeju Island. Monthly distributions (10^{th}, 50^{th} and 90^{th} percentiles) of the simulated afternoon mixing depths (Fig. 8(a)) indicated that from October through March (predominantly outflow conditions) the mixing depth varied from 400 to almost 2000 m, with median values ranging from 800 to 1200 m. May is at the end of the spring "outflow" period. It is also a time of frequent atmospheric near-stagnation events (e.g., Kim *et al.*, 2012), and has low mixing depths compared to other outflow months. The combination of these factors can lead to high pollution episodes late in the outflow season.

When interpreting emissions estimates made in subsequent sections, it is important to note that: (i) mean-monthly mixing depths were relatively consistent across the decade (typically varying by < 10%; Fig. 8(b)), and (ii) that, on average, there is a factor-of-four seasonal change in mixing depth at Gosan, which will be directly reflected in near-surface trace-gas concentrations.

Characterising "Background" Pollution Concentrations

To assess the efficacy of emission mitigation strategies, it is necessary to characterise temporal changes in local or regional net pollutant concentrations relative to the evolving large-scale (global or hemispheric) background signal. Background pollutant concentrations are unrelated to regional emissions, but may have seasonal or interannual variations.

Radon is an unambiguous indicator of the degree of terrestrial influence on an air mass over the past 2–3 weeks. Since the majority of anthropogenic pollution sources are of terrestrial origin, there is typically a close correspondence between radon concentration and atmospheric pollutants, or other natural trace species with terrestrial origins (e.g., Chambers *et al.*, 2016). Consequently, the most reliable estimates of background pollution levels are usually derived from air masses that have had the least recent land contact.

Figs. 9 and 10 demonstrate terrestrial influence on pollutants, using radon as a proxy. Only observations within the diurnal sampling window were used. "Outliers" (top and bottom 10%) of pollution concentrations within each 100 mBq m^{-3} radon "bin" were excluded prior to calculating statistics (μ, σ). Separate curves are shown for the beginning and end of the decade of observations as an indication of temporal change. Individual means and standard deviations were typically based on 10–90 hourly samples.

Although pollutant levels clearly decrease with decreasing terrestrial influence (radon), variability (σ) remained high for all radon bins. Since urban/industrial areas are often

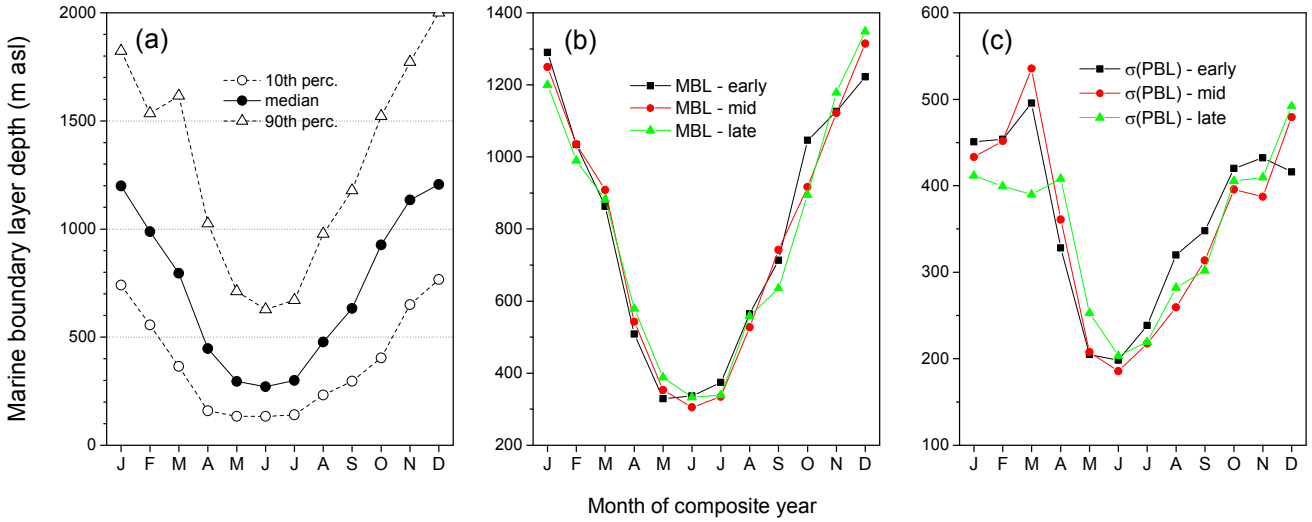

Fig. 8. Monthly distributions of afternoon mixing depths for the Gosan oceanic fetch as derived from the NCEP Climate Forecast System Reanalysis.

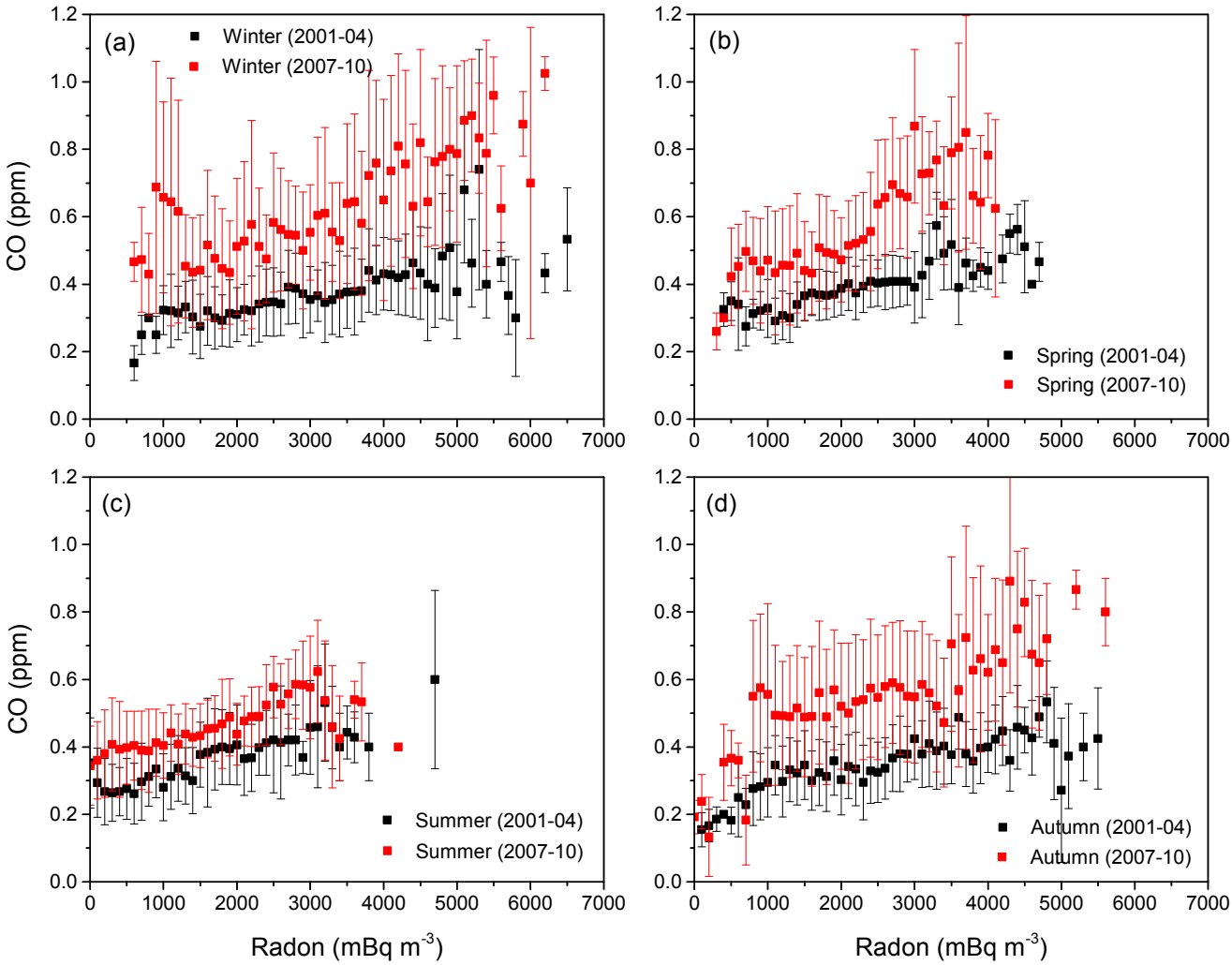

Fig. 9. Average CO within the diurnal sampling window as a function of increasing terrestrial influence (as indicated by radon), by season, for composite years at the beginning and end of the decade. Whiskers denote ±1 σ, radon "bin" size 100 mBq m^{-3}.

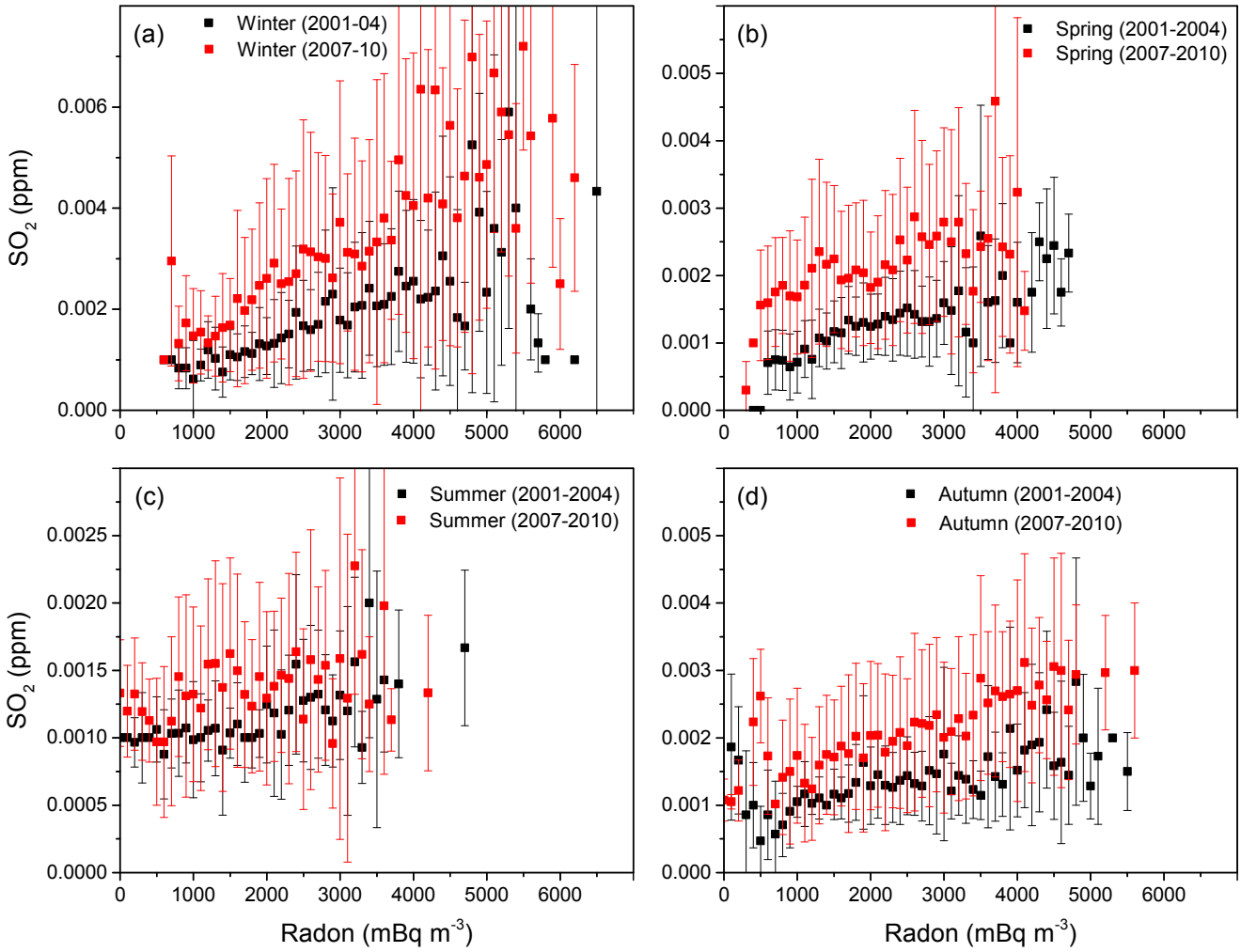

Fig. 10. As for Fig. 9 but for SO_2.

situated near the coast in SE Asia, it is possible for air masses to have only a brief "glancing" interaction with land (i.e., have a low radon concentration) and still accumulate significant levels of pollution before travelling to Gosan Station. Shipping activities in SE Asia are also a significant source of pollution (Guttikunda *et al.*, 2001). Conversely, an air mass may pass over sparsely populated regions of Siberia, Mongolia and North China (i.e., have a high radon value), and still arrive at Gosan station relatively unpolluted.

Air masses with low terrestrial influence (i.e., radon < 500 mBq m^{-3}) were observed in all seasons except winter. Taking the $\mu - 1\sigma$ pollution concentrations at low radon values to be representative of background air, in 2001–2004 background CO varied from 0.1 ppm in summer to ~0.2 ppm in the other seasons. In 2007–2010 the non-summer background CO concentration had increased slightly to ~0.25 ppm. For SO_2, on the other hand, background concentrations appeared to be near, or below, the 0.5 ppb detection limit across the decade for all seasons. Bin-mean SO_2 concentrations for the least terrestrially influenced air masses were very similar to the 1 ppb ambient concentrations for Gosan reported by Kim *et al.* (1998). The observed 0.05 ppm increase in non-summer background CO will be accounted for when emissions estimates are later compared across the decade. However, since background SO_2 concentrations remained near the instruments detection limit, no adjustment of the observed concentrations will be made.

It is of interest to note that the "cleanest" air masses were usually observed in the transition seasons. At these times the land-sea temperature gradient is weaker and air masses occasionally approach Gosan by looping up from the south, clockwise, and may have had no land contact for weeks.

Relating Observed Variability to Regional Emissions

Mean monthly CO and SO_2 values, based on observations in the diurnal sampling window (Figs. 11(a) and 11(c)), show both increasing trends over the decade and substantial inter-annual variability in the amplitude of the seasonal signal. This variability is unrelated to the small changes in "background" signal, discussed previously.

Annual mean CO was relatively constant from 2001–2004 (0.37 ± σ 0.009 ppm), but increased by > 30% in 2005–2009 (0.49 ± σ 0.05 ppm) and jumped to 0.69 ppm for 2010. While this increasing trend is in agreement with Gosan CO observations reported by Kim and Shon, (2011), it is in stark contrast to their findings for seven major cities on the

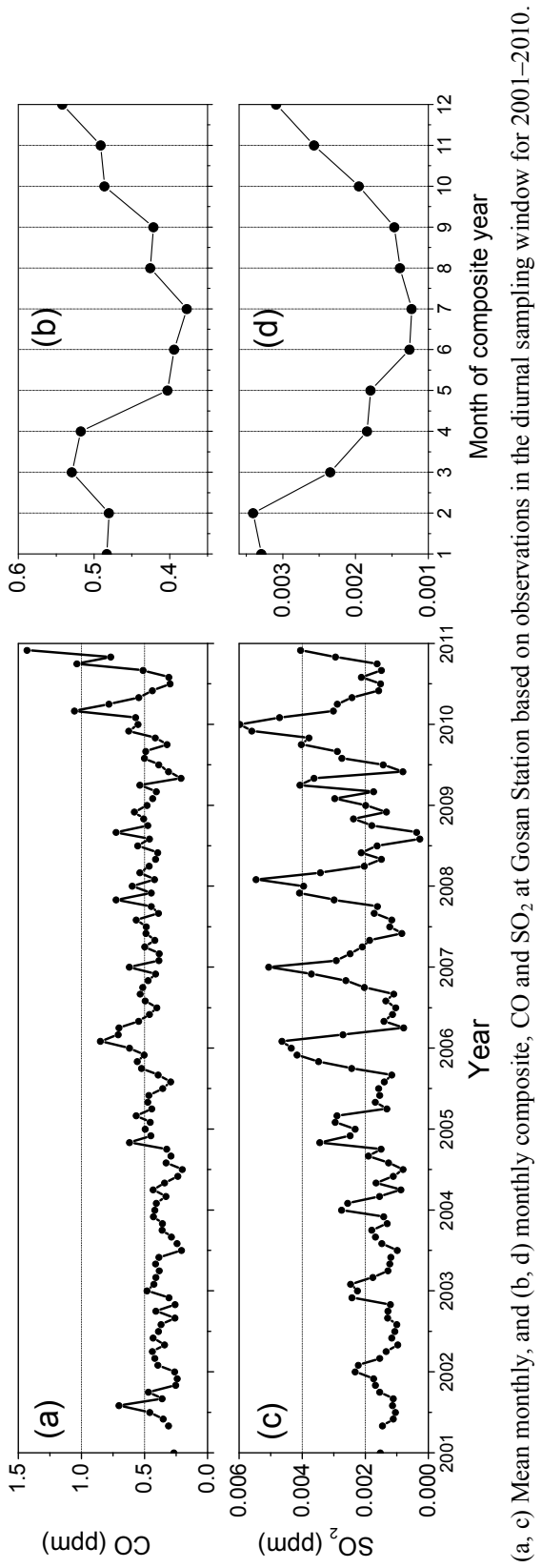

Fig. 11. (a, c) Mean monthly, and (b, d) monthly composite, CO and SO_2 at Gosan Station based on observations in the diurnal sampling window for 2001–2010.

Korean peninsula, which all showed a decreasing CO trend over the decade. Annual mean SO_2 concentrations increased steadily from 1.37 in 2001 to 2.25 ppb in 2006, held approximately steady for several years (± σ 0.06 ppb), and then rose to 2.91 ppb in 2009–2010 (Fig. 11(c)). Lu *et al.* (2010) also reported a slowing (even reduction) in SO_2 from China between 2006–2008 compared to earlier years.

Based on the whole decade, the composite seasonal cycles of CO and SO_2 (Figs. 11(b) and 11(d)) were generally characterised by higher values during continental Asian outflow conditions (Oct–Apr) and lower values between May and September. As well as the increased terrestrial influence (potential for pollution) in winter under outflow conditions, Streets *et al.* (2003) show that this is the time of peak fossil fuel combustion for power and heating.

The amplitudes of the seasonal signals (especially SO_2) have been changing markedly over the decade (Fig. 11). Variability as a result of (i) relative changes in terrestrial fetch regions, and (ii) time throughout the decade of observations, is discussed in the following sections.

Radon Variability

Considerable inter-annual variability (60% and 4% in annual minimum and maximum values, respectively) was evident in the long-term radon record (Fig. 3(a)). Due to the limited opportunity for pure oceanic fetch in summer (see Fig. 4), slight changes in regional flow patterns can result in large changes in radon. Factors contributing to changes in radon under outflow conditions include: (a) changing snow cover or soil moisture across continental Asia; (b) mean air mass fetch latitude (due to the Asian latitudinal flux gradient: Conen and Robertson, 2002; Zhuo *et al.*, 2008; Williams *et al.*, 2009); or (c) connectivity to surface sources (proportion of time an air mass has spent within the ABL). Since only monthly means are considered here, short-term influences on the radon flux (e.g., wind, pressure, and insolation) would likely be averaged out.

Changes in fetch and transport mechanisms that contribute to the natural inter-annual variability of radon shown in Fig. 3(a) may also be reflected, in part, in the pollutant observations. To minimise these effects on our estimates of pollution trends over the decade, we present subsequent results in three overlapping 4-year composite periods: Jan 2001–Dec 2004; Jan 2004–Dec 2007; and Jan 2007–Dec 2010, henceforth referred to as the "early", "middle" and "late" periods, respectively.

Temporal Changes in "Extreme" Pollution Events

Fig. 12 shows how the highest (> 90th percentile) pollution events recorded at Gosan changed over the decade. While more extreme in the case of SO_2, the seasonal cycle for both gases was characterised by winter maximum values (under Asian outflow conditions) and summer minimum values (during "onshore" regional flow). However, to fully appreciate the magnitude of this seasonal contrast it is necessary to consider the relative factor-of-four dilution of observed winter air masses (Fig. 8(b)).

Seasonal average "extreme" CO values (Fig. 12(b)) indicated a monotonic increase across the decade (~0.3

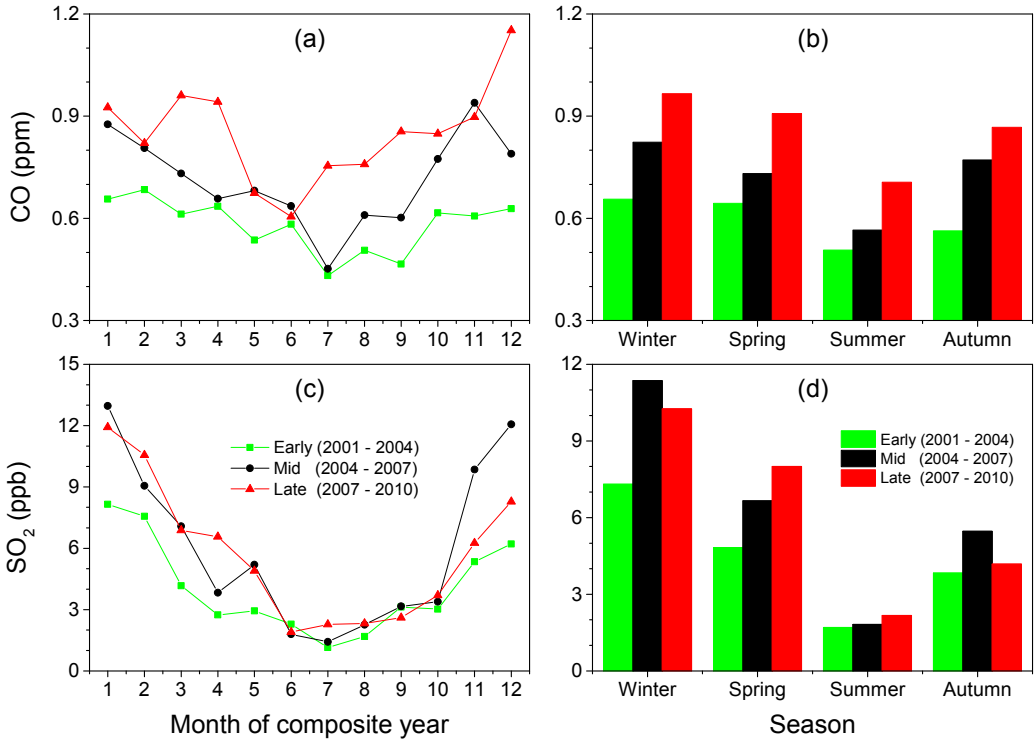

Fig. 12. Comparison of 90th percentile Gosan CO and SO_2 across the decade for (a, c) composite months, and (b, d) seasonal means of composite months. Note that the CO background has not been removed in these figures (see text for details).

ppm from early to late in the decade cf. the 0.05 ppm change in background CO). The monthly data, however, indicate particularly large recent increases in March–April, during the spring outflow period, and July-through-September. Apart from an increased fetch over Jeju in Jul–Sep, Fig. 5 indicates increased contributions from South China (July) and Japan (Aug–Sep).

For SO_2 a seasonal increase in "extreme" events across the decade was noted in spring and summer (Fig. 12(d)), when fetch was contributed to most significantly by South China (Fig. 5). Song *et al.* (2012) indicate a dense region of SO_2 emission toward the northern end of our "South China" fetch region, which has developed during the measurement period compared to the emissions map of Guttikunda *et al.* (2001). A range of technological improvements and abatement initiatives (including: flue gas desulfurization, improved coal quality, and strengthened emissions standards for power plants, cement plants and vehicles) were implemented across China between 2006–2008 (Lu *et al.*, 2010). However, Hu *et al.* (2014) claim that Chinese economic growth has outstripped emissions mitigations measures implemented between 2000 and 2011. For autumn and winter, however, when fetch contributions are more from North China and Korea, a slight reduction in SO_2 extreme events is evident in recent years. Since the seasonal CO extremes increased across the decade in winter and spring, contrary to the findings of Kim and Shon (2011) for mainland Korea, emissions from North China likely dominate observed concentrations at Gosan during these times; this is likely due to trajectories passing through North China fetch regions prior to crossing Korea. The slight reduction in SO_2 extremes over these seasons may then indicate that SO_2 emissions mitigation strategies midway through the decade (e.g., Lu *et al.*, 2010) were more effective for the lower-density industrial activity within the North China region. SO_2 observations at the nearby Anmyeon baseline station also indicate a reduction in concentrations between 2007–2010 compared to 2006 values (KMA, 2015; p.44).

Temporal Changes by Fetch Region Contributions

Figs. 13 and 14 show changes in mean-monthly pollutants from each of the terrestrial fetch regions (South China, North China, Korea and Japan) over the decade. Fig. 13 is based on all hourly observations, whereas Fig. 14 is based only on observations within the diurnal sampling window that also correspond to the upper 50% of radon concentrations from that fetch (i.e., observations considered most representative of the respective fetch regions). To facilitate intercomparison of the traditional and new sampling techniques, seasonal summaries are presented in Figs. 15 and 16.

For CO, the combination of techniques employed here to improve the representativeness of remote fetch regions mostly indicates that emissions from South China were higher than predicted based on averages of all hourly observations. By contrast, predicted emissions from the other fetch regions change very little, or are even less, than would be predicted using all hourly data.

For SO_2, our method again usually resulted in higher

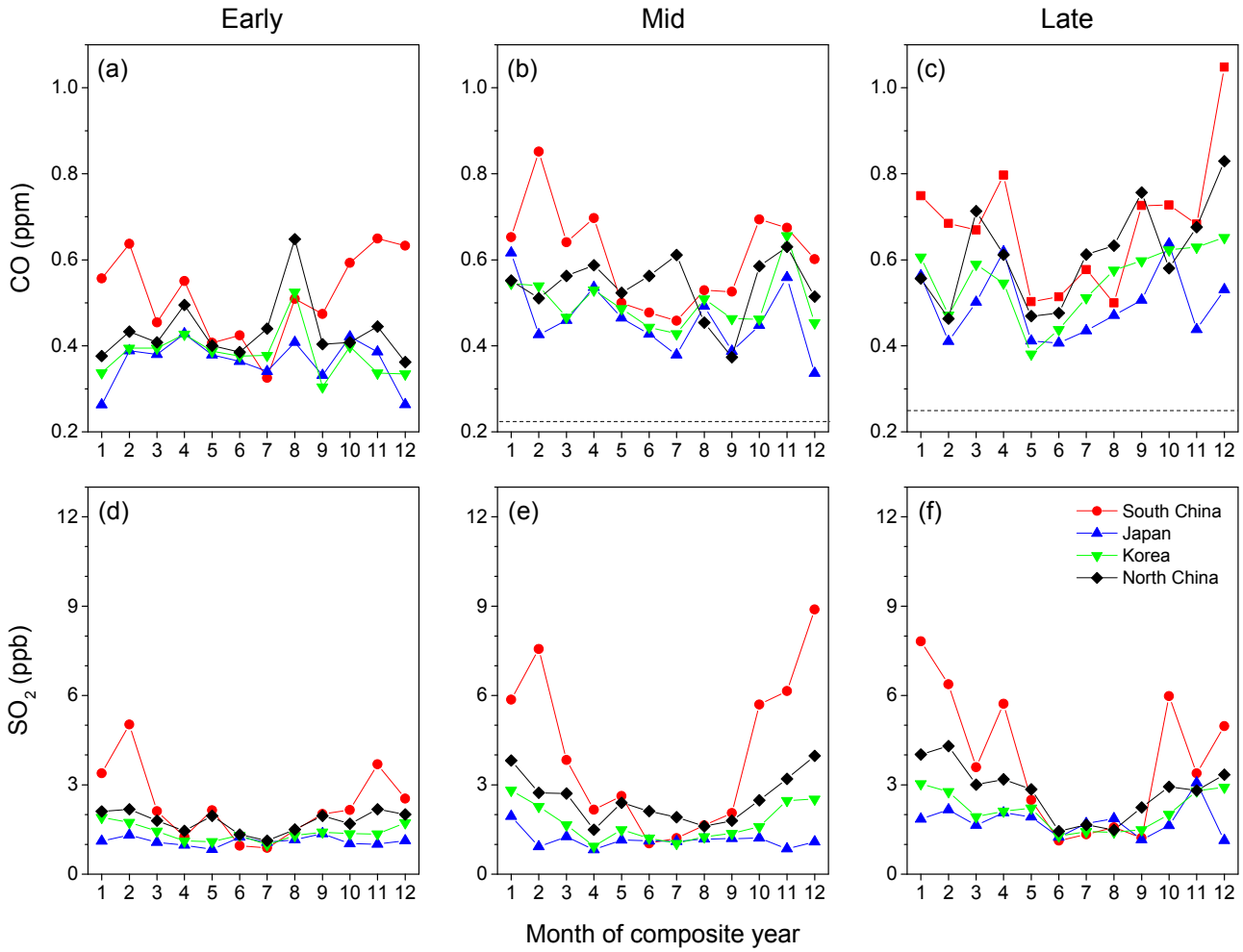

Fig. 13. Monthly-mean CO and SO_2 for each fetch region across the decade based on all hourly data. The background CO concentrations, gradually increasing above 0.2 ppm, are indicated by dotted lines.

values from South China than would otherwise be predicted using all hourly observations, and that pollution from Japanese fetch regions (whose corresponding air masses frequently pass over Jeju Island) would be similar, or slightly reduced. For Korean fetch in winter, however, our method predicts a slight increase in emissions compared to that based on all hourly data.

The above results indicate that unless local influences are minimised, and representative air masses sought, pollution estimates at Gosan from Japanese fetch would be overestimated. More importantly, perhaps, Figs. 14(d)–14(f) clearly demonstrate that the increase in amplitude of the SO_2 seasonal cycle evident in Fig. 11(c) is primarily attributable to a large SO_2 increase in winter "outflow" events from South China. Since there is no significant change in the winter-mean mean mixing depth across the decade (Fig. 8(b)), this increase (e.g. Fig. 16(b)) is completely attributable to a change in regional emissions.

Accounting for various loss mechanisms, it is estimated that approximately one third of the SO_2 produced in China actually leaves the borders (e.g., Guttikunda *et al.*, 2001). Assuming a 1% h^{-1} conversion rate to sulphate (Seinfeld and Pandis, 2006; and this study), and based on the 10^{th}/90^{th} percentile daytime wind speed at Gosan between October to April, a further 10–40% of this sulphur wouldbe lost *en route*. Sahu *et al.* (2009) estimated the SO_2 transport efficiency from China to Gosan in spring to be 40%. Consequently, column-integrated SO_2 estimates at Gosan may represent as little as 10–15% of the actual emissions from targeted fetch regions in China.

It is generally acknowledged that not all information regarding sources is consistent or reliable (Streets *et al.*, 2000; Akimoto *et al.*, 2006), and that not all emission sources are captured, or easy to accurately characterise (e.g., contributions from soils, agriculture, mobile sources, etc.). It will be a goal of future studies to combine the techniques described in this study with information regarding the seasonal variability in mixing depth at Gosan to better quantify the magnitude of regional emissions from the respective fetch regions.

CONCLUSIONS

We report on hourly atmospheric radon, CO, SO_2 and climatological observations made at the WMO GAW site Gosan Station, South Korea, over the period 2001–2010.

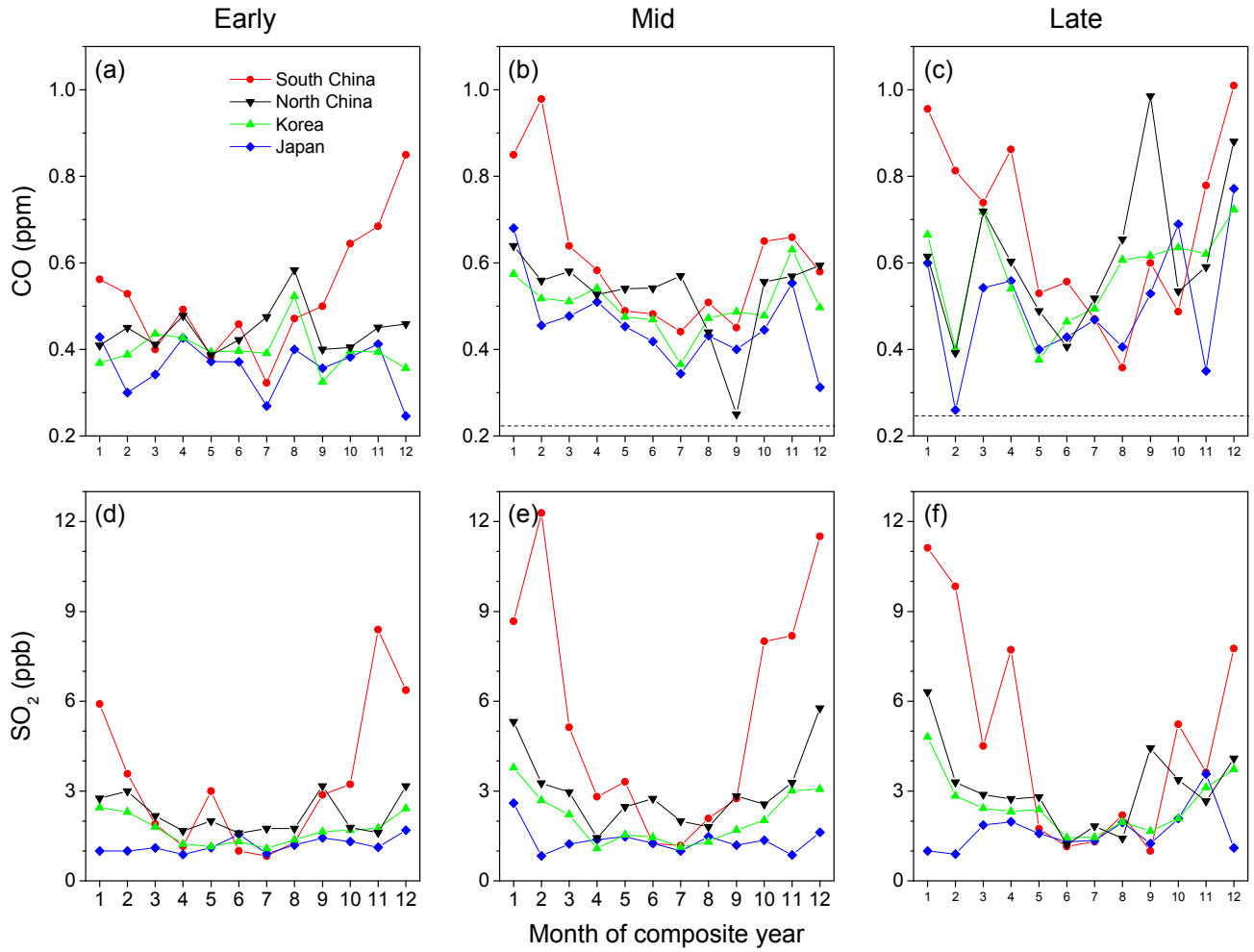

Fig. 14. Monthly-mean CO and SO_2 for each fetch region across the decade, based on measurements within the diurnal sampling window and corresponding to the upper 50% of radon concentrations (air masses most "well connected" to surface sources). Dotted lines indicate increasing background CO.

In July 2007 the original 750 L radon detector was replaced by an improved 1500 L model, coinciding with a 14% reduction in the mean annual concentrations but little change in the amplitude of the seasonal cycle. The performance of the two detectors is compared.

Since radon is an unambiguous indicator of terrestrial influence, and the majority of anthropogenic pollution sources are of terrestrial origin, we selected for analysis only those air masses corresponding to radon concentrations in the upper 50th percentile based on monthly distributions for each of four fetch regions: South China, North China, Korea and Japan. This approach ensures that sampled air masses have maintained consistent contact with the targeted fetch regions, and have not been substantially diluted by various atmospheric processes *en route* to the measurement site. Pollutant concentrations were also scrutinised as a function of terrestrial influence (using radon as a proxy) in order to characterise seasonal and longer-term variability in "background" pollutant concentrations.

Hourly radon concentrations were used to demonstrate the potential for contamination of remote-fetch pollution observations by local emissions at Gosan, and a seasonally-varying 5-hour diurnal sampling window is proposed for days on which diurnal cycles are evident in observations to avoid this issue.

Based on a subset of Gosan observations demonstrated to be most representative of remote fetch regions, seasonal estimates of CO and SO_2 in air masses originating from South China, North China, Korea and Japan are provided, and compared across the decade of observations. On average, across the whole measurement period, pollutant concentrations were highest in air masses originating from South China, and lowest in air masses whose dominant terrestrial influence was Japan. Compared to the selection techniques described here, traditional analysis methods underestimated pollution levels originating from emissions in north and south China, and overestimated levels from Japan. Generally, our selection technique was demonstrated to more accurately reflect known changes in SO_2 emissions from China over the decade of observations than results based on an analysis of all available hourly data.

SO_2 concentrations during wintertime continental "outflow" events were observed to increase markedly over the decade of measurements at Gosan. Through a

combination of our refined data selection technique, and analysis of MBL depth seasonality across the decade, we were able to attribute the bulk of this effect to an increase in emissions from South China. Employing these improved observations to improve regional emissions estimates will be the topic of a follow-up study.

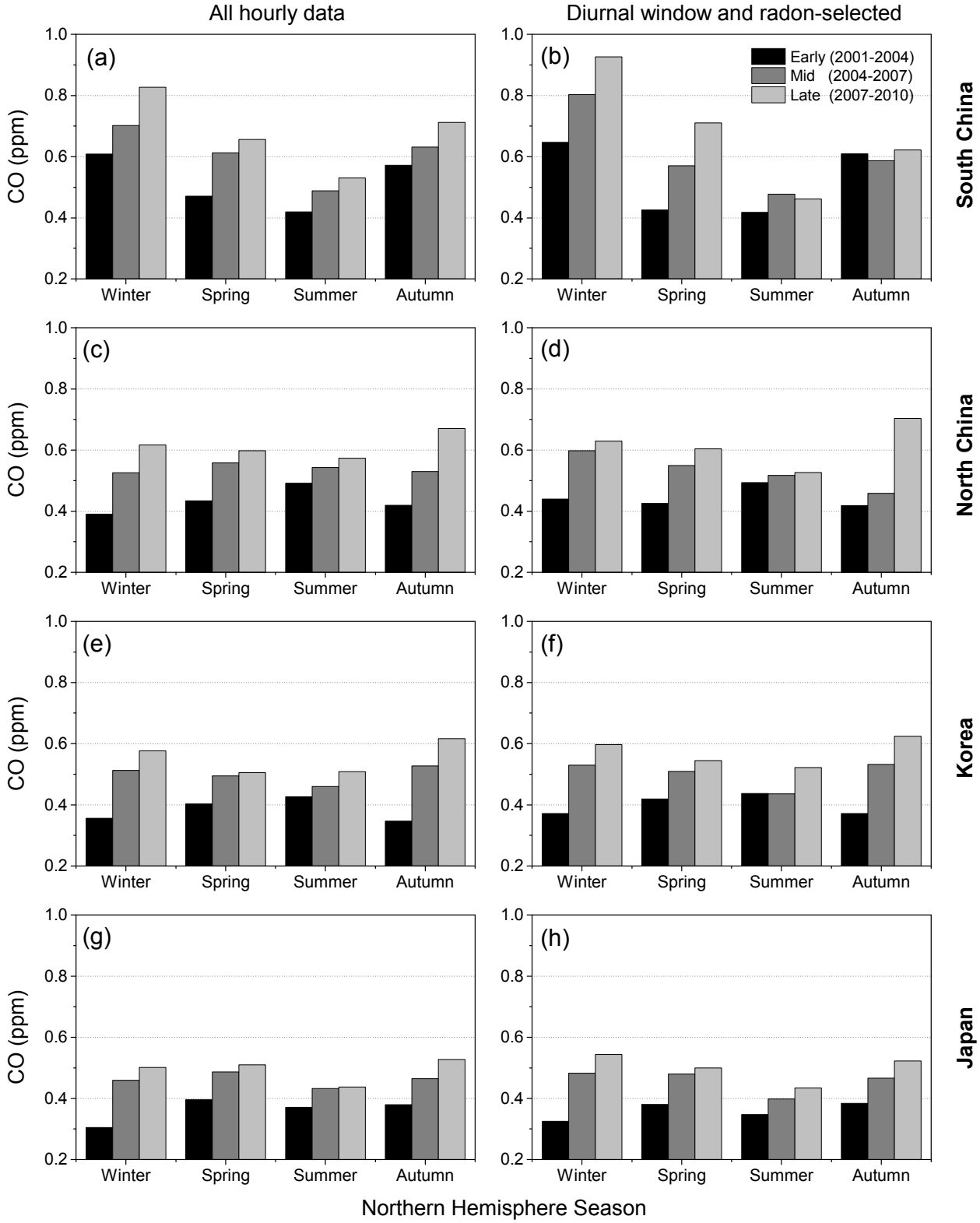

Fig. 15. Seasonal mean CO across the decade, by fetch region, based on (a, c, e, g) all hourly data, and (b, d, f, h) sampling method proposed in this study. Ordinate scale set to "early" CO background (an additional 0.025 or 0.05 ppm needs to be removed from the "mid" and "late" results).

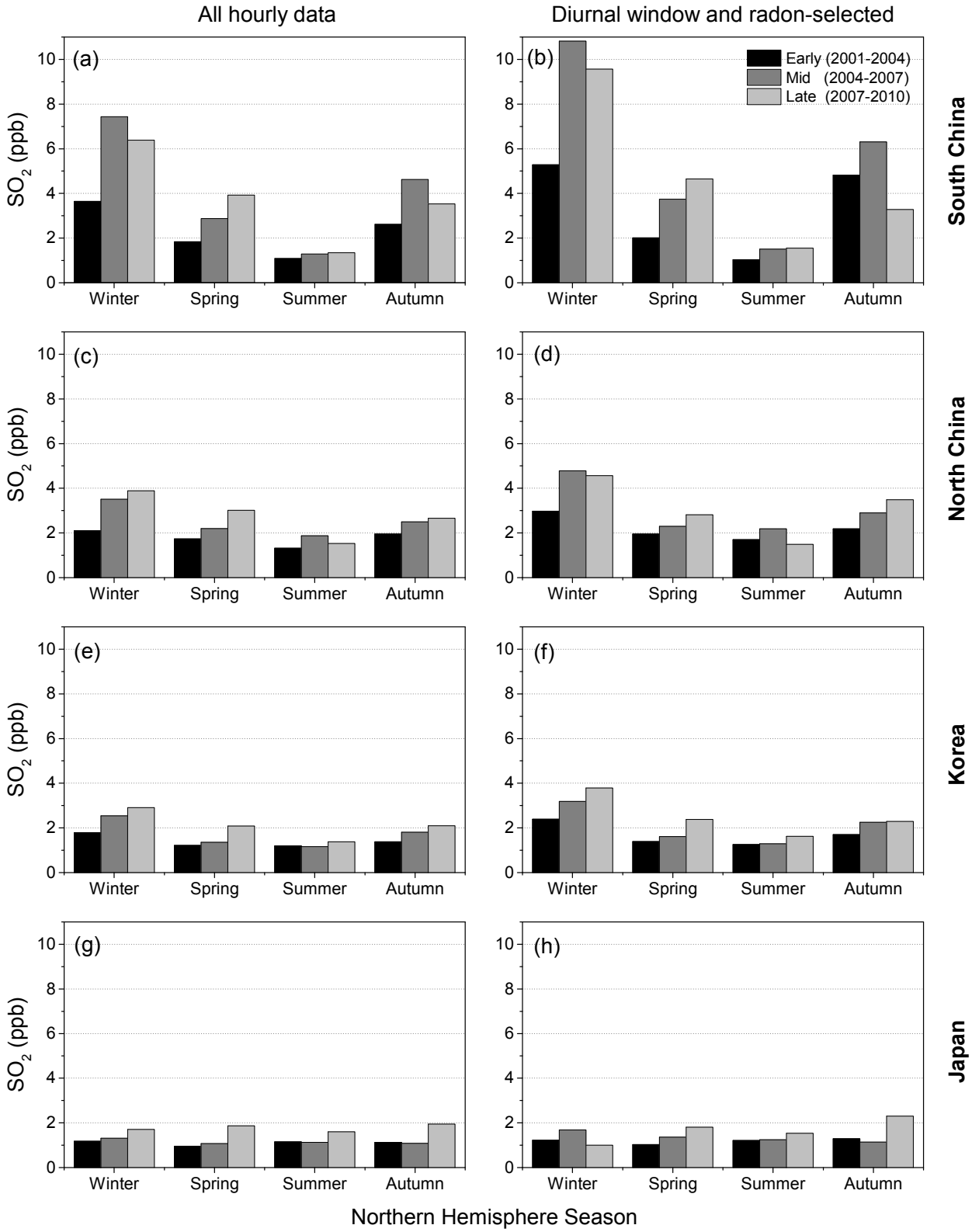

Fig. 16. As for Fig. 15 but for SO_2.

ACKNOWLEDGMENTS

The authors wish to thank Ot Sisoutham and Sylvester Werczynski at the Australian Nuclear Science and Technology Organisation for their support of the radon measurement program at Gosan Station. This work was funded by the Korea Meteorological Administration Research and Development Program under Grant KMIPA

2015-2050, and we gratefully acknowledge the use of sulphur dioxide and carbon monoxide data monitored by the Korean Ministry of Environment. Also, the NOAA Air Resources Laboratory (ARL), for providing the HYSPLIT v4 transport and dispersion model and relevant input files for generation of back trajectories. KHK acknowledges partial support made by a grant from the National Research Foundation of Korea (NRF) funded by the Ministry of Education, Science and Technology (MEST) (No. 2009-0093848).

REFERENCES

Akimoto, H., Ohara, T. Kurokawa, J.I. and Horii, N. (2006). Verification of Energy Consumption in China during 1996–2003 by Using Satellite Observational Data. *Atmos. Environ.* 40: 7663–7667.

Balkanski, Y.J., Jacob, D.J., Arimoto, R. and Kritz, M.A. (1992). Distribution of ^{222}Rn over the North Pacific: Implications for Continental Influences. *J. Atmos. Chem.* 14: 353–374.

Begum, B.A., Biswas, S.K., Pandit, G.G., Saradhi, IV., Waheed, S. Siddique, N., Seneviratne, M.C.S., Cohen, D.D., Markwitz, A. and Hopke, P.K. (2011). Long–range Transport of Soil Dust and Smoke Pollution in the South Asian Region. *Atmos. Pollut. Res.* 2: 151–157.

Carmichael, G.R., Hong, M.S., Ueda, H., Chen, L.L., Murano, K., Park, J.K., Lee, H.G., Kim, Y., Kang, C. and Shim, S. (1997). Aerosol Composition at Cheju Island, Korea. *J. Geophys. Res.* 102: 6047–6061.

Chambers, S.D., Wang, F., Williams, A.G., Xiaodong, D., Zhang, H., Lonati, G., Crawford, J., Griffiths, A.D., Ianniello, A. and Allegrini, I. (2015a). Quantifying the Influences of Atmospheric Stability on Air Pollution in Lanzhou, China, Using a Radon-based Stability Monitor. *Atmos. Environ.* 107: 233–243.

Chambers, S.D., Williams, A.G., Crawford, J. and Griffiths, A.D. (2015b). On the Use of Radon for Quantifying the Effects of Atmospheric Stability on Urban Emissions. *Atmos. Chem. Phys.* 15: 1175–1190.

Chambers, S.D., Hong, S.B., Williams, A.G., Crawford, J., Griffiths, A.D. and Park, S.J. (2014). Characterising Terrestrial Influences on Antarctic Air Masses Using Radon-222 Measurements at King George Island. *Atmos. Chem. Phys.* 14: 9903–9916.

Chambers, S.D., Williams, A.G., Conen, F., Griffiths, A.D., Reimann, S., Steinbacher, M., Krummel, P.B., Steele, L.P., van der Schoot, M.V., Galbally, I.E., Molloy, S.B. and Barnes, J.E. (2016). Towards a Universal "Baseline" Characterisation of Air Masses for High- and Low-altitude Observing Stations Using Radon-222. *Aerosol Air Qual. Res.* 16: 885–899, doi: 10.4209/aaqr.2015.06.0391.

Choi, I.J., Kim, S.W., Kim, J., Yoon, S.C., Kim, M.H., Sugimoto, N., Kondo, Y., Miyazaki, Y., Moon, K.J. and Han, J.S. (2008). Characteristics of the Transport and Vertical Structure of Aerosols during ABC-EAREX2005. *Atmos. Environ.* 42: 8513–8523.

Conen, F. and Robertson, L.B. (2002). Latitudinal Distribution of Radon-222 Flux from Continents. *Tellus Ser. B* 54: 127–133.

Crawford, J., Zahorowski, W. and Cohen, D.D. (2009). A New Metric Space Incorporating Radon-222 for Generation of Back Trajectory Clusters in Atmospheric Pollution Studies. *Atmos. Environ.* 43: 371–381.

Crawford, J., Davis, D., Chen, G., Bradshaw, J., Sandholm, S., Kondo, Y., Liu, S., Browell, E., Gregory, G., Anderson, B., Sachse, G., Collins, J., Barrick, J., Blake, D., Talbot, R. and Singh, H. (1997). An Assessment of Ozone Photochemistry in the Extratropical Western North Pacific: Impact of continental Outflow during the Late Winter/Early Spring. *J. Geophys. Res.* 102: 28469–28487.

Crawford, J., Chambers, S., Cohen, D.D., Dyer, L., Wang, T. and Zahorowski, W. (2007). Receptor Modelling Using Positive Matrix Factorisation, Back Trajectories and Radon-222. *Atmos. Environ.* 41: 6823–6837.

Crawford, J., Chambers, S., Kang, C.H., Griffiths, A. and Kim, W.H. (2015). Analysis of a Decade of Asian Outflow of PM_{10} and TSP to Gosan, Korea; also Incorporating Radon-222. *Atmos. Pollut. Res.* 6: 529–539.

Guttikunda, S.K., Thongboonchoo, N., Arndt, R.L., Calori, G., Carmichael, G.R. and Streets, D.G. (2001). Sulfur Deposition in Asia: Seasonal Behaviour and Contributions from Various Energy Sectors. *Water Air Soil Pollut.* 131: 383–406.

Hu, H., Zhang, X.H. andLin, L.L. (2014). The Interactions between China'S Economic Growth, Energy Production and Consumption and the Related Air Emissions during 2000-2011. *Ecol. Indic.* 46: 38–51.

Huebert, B.J., Bates, T., Russell, P.B., Guangyu, S., Young, J.K., Kawamura, K., Carmichael, G. and Nakajima, T. (2003). An Overview of ACE-Asia: Strategies for Quantifying the Relationships between Asian Aerosols and their Climatic Impacts. *J. Geophys. Res.* 108: 8633–8633.

Kang, C.H., Kim, W.H., Ko, H.J. and Hong, S.B. (2009). Asian Dust Effects on Total Suspended Particulate (TSP) Compositions at Gosan in Jeju Island, Korea. *Atmos. Res.* 94: 345–355.

Kim, J., Yoon, S.C., Jefferson, A., Zahorowski, W. and Kang, C.H. (2005). Air Mass Characterization and Source Region Analysis for the Gosan Super-site, Korea, during the ACE-Asia 2001 Field Campaign. *Atmos. Environ.* 39: 6513–6523.

Kim, J., Jung, C.H., Choi, B.C., Oh, S.N., Brechtel, F.J., Yoon, S.C. and Kim, S.W. (2007a). Number Size Distribution of Atmospheric Aerosols during ACE-Asia Dust and Precipitation Events. *Atmos. Environ.* 41: 4841–4855.

Kim, J.Y., Kim, S.W., Ghim, Y.S., Song, C.H. and Yoon, S.C. (2012). Aerosol Properties at Gosan in Korea during Two Pollution Episodes Caused by Contrasting Weather Conditions. *J. Atmos. Sci.* 48: 25–33.

Kim, K.H. and Shon, Z.H. (2011). Nationwide Shift in CO Concentration Levels in Urban Areas of Korea after 2000. *J. Hazard. Mater.* 188: 235–246.

Kim, N.K., Kim, Y.P. and Kang, C.H. (2011). Long-term

Trend of Aerosol Composition and Direct Radiative Forcing Due to Aerosols over Gosan: TSP, PM_{10}, and $PM_{2.5}$ Data between 1992 and 2008. *Atmos. Environ.* 45: 6107–6115.

Kim, S.W., Yoon, S.C., Kim, J. and Kim, S.Y. (2007b). Seasonal and Monthly Variations of Columnar Aerosol Optical Properties over East Asia Determined from Multi-year MODIS, LIDAR, and AERONET Sun/Sky Radiometer Measurements. *Atmos. Environ.* 41: 1643–1651.

Kim, W.H., Ko, H.J., Hu, C.G., Lee, H., Lee, C., Chambers, S., Williams, A.G. and Kang, C.H. (2014b). Background Level of Atmospheric Radon-222 Concentrations at Gosan Station, Jeju Island, Korea in 2011. *Bull. Korean Chem. Soc.* 35: 1149, doi: 10.5012/bkcs.2014.35.4.1149.

Kim, Y., Kim, S.W. Yoon, S.C., Kim, M.H. and Park, K.H. (2014a). Aerosol Properties and Associated Regional Meteorology during Winter Pollution Event at Gosan Climate Observatory, Korea. *Atmos. Environ.* 85: 9–17.

Kim, Y.P., Shim, S.G., Moon, K.C., Baik, N.J., Kim, S.J. Hu, C.G. and Kang, C.H. (1995). Characteristics of Particles at Kosan, Cheju Island: Intensive Study Results during March 11–17 (in Korean). *J. Korea Air Pollut. Res. Assoc.* 11: 263–272.

Kim, Y.P., Shim, S.G., Moon, K.C., Hu, C.G., Kang, C.H. and Park, K.Y. (1998). Monitoring of Air Pollutants at Kosan, Cheju Island, Korea, during March–April 1994. *J. Appl. Meteorol.* 37: 1117–1126.

KMA (2015). Report of Global Atmosphere Watch, 2014 (in Korean). Annual report of the Korea Meteorological Administration, KMA 11-1360000-000991-10, 292 pp. https://drive.google.com/file/d/0BziYuet7Hu4dMXRxWkNmNFFfT0U/view?usp=sharing.

Kritz, M.A., Le Roulley, J.C. and Danielsen, E.F. (1990). The China Clipper—Fast Advective Transport of Radon-rich Air from the Asian Boundary Layer to the Upper Troposphere near California. *Tellus Ser. B* 42: 46–61.

Lin, M., Oki, T., Holloway, T., Streets, D.G., Bengtsson, M. and Kanae, S. (2008). Long-range Transport of Acidifying Substances in East Asia—Part I Model Evaluation and Sensitivity Studies. *Atmos. Environ.* 42: 5939–5955.

Liu, S.C., McAfee, J.R. and Cicerone, R.J. (1984). Radon 222 and Tropospheric Vertical Transport. *J. Geophys. Res.* 89: 7291–7297.

Lu, Z., Streets, D.G., Zhang, Q., Wang, S., Carmichael, G.R., Cheng, Y.F., Wei, C., Chin, M., Diehl, T. and Tan, Q. (2010). Sulphur Dioxide Emissions in China and Sulphur Trends in East Asia Since 2000. *Atmos. Chem. Phys.* 10: 6311–6331.

Nakajima, T., Yoon, S., Ramanathan, V., Shi, G., Takemura, T., Higurashi, A., Takamura, T., Aoki, K., Sohn, B., Kim, S., Tsuruta, H., Sugimoto, N., Shimizu, A., Tanimoto, H., Sawa, Y., Lin, N., Lee, C., Goto, D. and Schutgens, N. (2007). Overview of the Atmospheric Brown Cloud East Asian Regional Experiment 2005 and a study of the Aerosol Direct Radiative Forcing in East Asia. *J. Geophys. Res.* 112: D24S91, doi: 10.1029/2007JD009009.

Park, M.H., Kim, Y.P., Kang, C.H. and Shim, S.G. (2004). Aerosol Composition Change between 1992 and 2002 at Gosan, Korea. *J. Geophys. Res.* 109: D19S13.

Perry, K.D., Cahill, T.A., Schnell, R.C. and Harris, J.M. (1999). Long-range Transport of Anthropogenic Aerosols to the National Oceanic and Atmospheric Administration Baseline Station at Mauna Loa Observatory, Hawaii. *J. Geophys. Res.* 104: 18521–18533.

Reid, J.S., Hyer, E.J., Johnson, R.S., Holben, B.N., Yokelson, R.J., Zhang, J., Campbell, J.R., Christopher, S.A., Di Girolamo, L., Giglio, L., Holz, R.E., Kearney, C., Miettinen, J., Reid, E.A., Turk, F.J., Wang, J., Xian, P., Zhao, G., Balasubramanian, R., Chew, B.N., Janjai, S., Lagrosas, N., Lestari, P., Lin, N.H., Mahmud, M., Nguyen, A.X., Norris, B., Oanh, N.T.K., Oo, M., Salinas, S.V., Welton, E.J. and Liew, S.C. (2013). Observing and Understanding the Southeast Asian Aerosol System by Remote Sensing: An Initial Review and Analysis for the Seven Southeast Asian Studies (7SEAS) Program. *Atmos. Res.* 122: 403–468.

Saha, S., Moorthi, S., Pan, H.L., Wu, X., Wang, J., Nadiga, S., Tripp, P., Kistler, R., Woollen, J., Behringer, D., Liu, H., Stokes, D., Grumbine, R., Gayno, G., Wang, J., Hou, Y.T., Chuang, H.Y., Juang, H.M.H., Sela, J., Iredell, M., Treadon, R., Kleist, D., Delst, P.V., Keyser, D., Derber, J., Ek, M., Meng, J., Wei, H., Yang, R., Lord, S., van den Dool, H., Kumar, A., Wang, W., Long, C., Chelliah, M., Xue, Y., Huang, B., Schemm, J.K., Ebisuzaki, W., Lin, R., Xie, P., Chen, M., Zhou, S., Higgins, W., Zou, C.Z., Liu, Q., Chen, Y., Han, Y., Cucurull, L., Reynolds, R.W., Rutledge, G. and Goldberg, M. (2010). NCEP Climate Forecast System Reanalysis (CFSR) Selected Hourly Time-Series Products, January 1979 to December 2010. Research Data Archive at the National Center for Atmospheric Research, Computational and Information Systems Laboratory. doi: 10.5065/D6513W89, Last Access: 1 Aug 2013.

Saha, S., Moorthi, S., Pan, H. L., Wu, X., Wang, J., Nadiga, S., Tripp, P., Kistler, R., Woollen, J. and Behringer, D. (2010). The NCEP Climate Forecast System Reanalysis. *Bull. Am. Meteorol. Soc.* 91: 1015–1057.

Sahu, L.K., Kondo, Y., Miyazaki, Y., Kuwata, M., Koike, M., Takegawa, N., Tanimoto, H., Matsueda, H., Yoon, S.C. and Kim, Y.J. (2009). Anthropogenic Aerosols Observed in Asian Continental Outflow at Jeju Island, Korea, in Spring 2005. *J. Geophys. Res.* 114: D03301, doi: 10.1029/2008JD010306.

Seinfeld, J.H. and Pandis, S.N. (2006). *Atmospheric Chemistry and Physics: From Air Pollution to Climate Change*, 2nd Edn., John Wiley & Sons, Inc., Hoboken, New Jersey, USA.

Song, C.H., Nam, J.E., Han, K.M., Lee, M.K., Woo, J.H. and Han, J.S. (2012). Influence of Mineral dust Mixing-state and Reaction Probabilities on Size-resolved Sulfate Formation in Northeast Asia. *Atmos. Environ.* 58: 23–34.

Song, S.K., Kim, Y.K., Shon, Z.H. and Lee, H.W. (2008). Influence of Meteorological Conditions on Trans-Pacific Transport of Asian dust during Spring Season. *J. Aerosol Sci.* 39: 1003–1017.

Streets, D.G., Tsai, N.Y., Akimoto, H. and Oka, K. (2000).

Sulfur Dioxide Emissions in Asia in the Period 1985–1997. *Atmos. Environ.* 34: 4413–4424, doi: 10.1016/S1352-2310(00)00187-4.

Streets, D.G., Bond, T.C., Carmichael, G.R., Fernandes, S.D., Fu, Q., He, D., Klimont, Z., Nelson, S.M., Tsai, N.Y., Wang, M.Q., Woo, J.H. and Yarber, K.F. (2003). An Inventory of Gaseous and primary Aerosol Emissions in Asia in the Year 2000. *J. Geophys. Res.* 108: 8809, doi: 10.1029/2002JD003093.

Talbot, R.W., Dibb, J.E., Lefer, B.L., Bradshaw, J.D., Sandholm, S.T., Blake, D.R., Blake, N.J., Sachse, G.W., Collins, J.E., Heikes, B.G., Merrill, J.T., Gregory, G.L., Anderson, B.E., Singh, H.B., Thornton, D.C., Bandy, A.R. and Pueschel, R.F. (1997). Chemical Characteristics of Continental Outflow from Asia to the Troposphere over the Western Pacific Ocean during February–March 1994: Results from PEM-West B. *J. Geophys. Res.* 102: 28255–28274.

Weinstock, B. (1969). Carbon monoxide: residence time in the Atmosphere. *Science* 166: 224–225.

Whittlestone, S. and Zahorowski, W. (1998). Baseline Radon Detectors for Shipboard Use: Development and Deployment in the First Aerosol Characterisation Experiment (ACE 1). *J. Geophys. Res.* 103: 16743–16751.

Williams, A.G., Chambers, S., Zahorowski, W., Crawford, J., Matsumoto, K. and Uematsu, M. (2009). Estimating the Asian Radon Flux Density and its Latitudinal Gradient in Winter Using Ground-based Radon Observations at Sado Island. *Tellus Ser. B* 61: 732–746.

Williams, A.G., Zahorowski, W., Chambers, S., Griffiths, A., Hacker, J.M., Element, A. and Werczynski, S. (2011). The Vertical Distribution of Radon in Clear and Cloudy Daytime Terrestrial Boundary Layers. *J. Atmos. Sci*. 68: 155–174.

Williams, A.G., Chambers, S.D. and Griffiths, A. (2013). Bulk Mixing and Decoupling of the Nocturnal Stable Boundary Layer Characterized Using a Ubiquitous Natural Tracer. *Boundary Layer Meteorol.* 149: 381–402, doi: 10.1007/s10546-013-9849-3.

Zahorowski, W., Chambers, S., Wang, T., KANG, C.H., Uno, I., Poon, S., Oh, S.N., Werczynski, S., Kim, J. and Henderson-Sellers, A. (2005). Radon-222 in Boundary Layer and Free Tropospheric Continental Outflow Events at Three ACE-Asia Sites. *Tellus Ser. B* 57: 124–140.

Zahorowski, W., Griffiths, A.D., Chambers, S.D., Williams, A.G., Law, R.M., Crawford, J. and Werczynski, S. (2013). Constraining Annual and Seasonal Radon-222 Flux Density from the Southern Ocean Using Radon-222 Concentrations in the Boundary Layer at Cape Grim. *Tellus Ser. B* 65: 19622, doi: 10.3402/tellusb.v65i0.19622.

Zhang, M., Uno, I., Yoshida, Y., Xu, Y., Wang, Z., Akimoto, H., Bates, T., Quinn, T., Bandy, A. and Blomquist, B. (2004). Transport and Transformation of Sulfur Compounds over East Asia during the TRACE-P and ACE-Asia Campaigns. *Atmos. Environ.* 38: 6947–6959.

Zhang, Q., Streets, D.G., Carmichael, G.R., He, K.B., Huo, H., Kannari, A., Klimont, Z., Park, I.S., Reddy, S., Fu, J.S., Chen, D., Duan, L., Lei, Y., Wang, L.T. and Yao, Z.L. (2009). Asian Emissions in 2006 for the NASA INTEX-B Mission. *Atmos. Chem. Phys.* 9: 5131–5153, doi: 10.5194/acp-9-5131-2009.

Zhu, C., Yoshikawa-Inoue, H., Matsueda, H., Sawa, Y., Niwa, Y., Wada, A. and Tanimoto, H. (2012). Influence of Asian Outflow on Rishiri Island, Northernmost Japan: Application of Radon as a Tracer for Characterizing Fetch Regions and Evaluating a Global 3D Model. *Atmos. Environ.* 50: 174–181.

Zhuo, W.H., Guo, Q.J., Chen, B. and Cheng, G. (2008). Estimating the Amount and Distribution of Radon Flux Density from the Soil Surface in China. *J. Environ. Radioact*. 99: 1143–1148.

Received for review, August 27, 2015
Revised, October 29, 2015
Accepted, October 29, 2015